SECONDARY STRUCTURAL ANALYSIS OF *SHIGELLA FLEXNERI* INVASION PLASMID ANTIGEN B (IPAB)

By

CHRISTOPHER MICHAEL SHEEHAN

Bachelor of Science in Microbiology

Oklahoma State University

Stillwater, Oklahoma

2007

Submitted to the Faculty of the
Graduate College of
Oklahoma State University
in partial fulfillment of
the requirements for
the Degree of
MASTER OF SCIENCE
May, 2010

SECONDARY STRUCTURAL ANALYSIS OF

SHIGELLA FLEXNERI INVASION

PLASMID ANTIGEN B (IPAB)

Thesis Approved:

Dr. Wendy Picking

Thesis Adviser

Dr. William Picking

Dr. Ed Shaw

Dr. A. Gordon Emslie

Dean of the Graduate College

ACKNOWLEDGMENTS

I would like to thank my adviser, Dr. Wendy Picking for allowing me to work in her lab and for her guidance. I want to thank my committee members, Dr. William Picking and Dr. Ed Shaw, for their support and input concerning my research. I owe many thanks to the members of the Picking lab who were always helpful and very giving of their time. I would like to thank my wife for understanding and always being there when I need her.

TABLE OF CONTENTS

LIST OF TABLES

Table Page

LIST OF FIGURES

Figure Page

CHAPTER I

INTRODUCTION

Millions of people around the world are affected by diarrheal diseases every year. *Shigella flexneri* is a gram-negative facultative anaerobic bacillus that is the causative agent of shigellosis, a severe form of bacillary dysentery. The largest number of cases are found in developing countries due to endemic infections by *Shigella* spp, however, approximately 14,000 cases a year are reported in the United States to the Centers for Disease Control and Prevention (http://www.cdc.gov/nczved/dfbmd/disease_listing/shigellosis_gi.html). This number is thought to be significantly underestimated, and the actual number may be as much as twenty times more since infections with *Shigella* spp. not required to be reported and there are many undiagnosed cases (http://www.cdc.gov/nczved/dfbmd/disease_listing/shigellosis_gi.html). The large number of people affected around the world, the many deaths it is responsible for and the emergence of antibiotic drug resistant strains have led to increased interest in a possible vaccine for *Shigella flexneri*.

Historical Review

Kiyoshi Shiga was the first to characterize the etiological agent of bacillary dysentery while studying the sekiri (dysentery) outbreaks in Japan in 1897 (Shiga, 1897). While working at the Institute of Infectious Diseases in Japan, he isolated bacilli from the stools of thirty-six dysentery patients under observation (Shiga, 1897). This bacillus was gram-negative, a dextrose fermenter, had a negative indole reaction and was unable to form acid from mannitol (Niyogi, 2005). He found this bacillus also caused diarrhea when it was subcultured and fed to dogs (Niyogi, 2005). While continuing to characterize the organism, Shiga first named it *Bacillus dysenteriae* (Shiga, 1906). Soon after Shiga's initial observation of *Bacillus dysenteriae,* other investigators were working to characterize this newly discovered organism. Several of these investigators discovered organisms morphologically and biochemically similar to the *Bacillus dysenteriae* reported by Shiga that caused similar disease in patients (Flexner, 1900) (Kruse, 1900).

During the next forty years, the genus *Shigella* grew to include three additional groups of related organisms, *S. flexneri*, *S. boydii*, and *S. sonnei* along with *S. dysenteria*, all named in honor of their lead workers, Flexner, Boyd, Sonne and Shiga (Hale, 1991). The genus *Shigella* was first named in the 1930 edition of *Bergey's Manual of Determinative Bacteriology,* but was officially adopted by the 1952 Congress of the International Association of Microbiologists (*Shigella* Commission) (Niyogi, 2005). The bacteria Shiga initially discovered became known as *Shigella dysenteriae* type 1 (http://www.about-shigella.com/).

The genus *Shigella* currently includes the four species previously named and belongs to the family Enterobacteriaceae. Biochemical and serological differences are the basis of the classification of the four species, with each composing a different serogroup, A, B, C and D (Niyogi, 2005).

Beginning in the 1950's, shigellae investigators shifted their focus to determining the mechanism of virulence. The host range of *Shigella* is small, consisting of humans and other higher primates; however, in the 1950s animal model was discovered when the corneal epithelium of guinea pigs were infected with *Shigella* spp. (Sereńy test) (Sereńy, 1957). Not long after in the early 1960s, *Shigella* spp. were shown to possess the ability to grow in cultured mammalian cells (Gerber and Watkins, 1961).

Into the 1960s, many researchers believed the release of toxins by shigellae when adhered to the surface of intestinal epithelial cells was its main source of pathogenicity (Watkins, 1960). However, work done by LaBrec *et al.* established that shigellosis required the invasion of the colonic epithelium (LaBrec *et al.*, 1964). They observed that ulceration and penetration of the epithelial cells of the colon and lamina propia resulted when guinea pigs were fed virulent strains of *S. flexneri* (LaBrec *et al.*, 1964).

In the 1980s, Sansonetti and his colleagues discovered that a large plasmid was the genetic basis for the pathogensis of the shigellae (Sansonetti, 1981). They showed that a loss of this plasmid made the organism unable to invade cultured mammalian cells or induce keratoconjunctivitis, inflammation of cornea and conjunctiva, in guinea pigs (Sansonetti, 1981) (Sansonetti, 1982).

This large, 200-kb plasmid has been shown to contain the necessary genes required for invasion by *Shigella* and it has been found in all four species (Buchrieser *et al.*, 2000). Currently, many *Shigella* researchers are focused on the characterization of this large plasmid to better understand the genes it contains and the proteins it encodes.

Epidemiology and Pathology

Shigellosis is a common disease of humans with infection mostly limited to the intestinal mucosa (Niyogi, 2005). Its symptoms include watery diarrhea with mucus, fever, malaise, and abdominal cramping (Niyogi, 2005). Ulceration of the mucosa may also result in bloody mucoid stools and/or fembrile diarrhea (Niyogi, 2005). The species and the number of organisms ingested determine the severity and range of symptoms expressed by an infected person. It has been shown that persons with conditions such as septicemia, bacteremia, dehydration, hypoglycemia, uremic and hemolytic syndrome, and toxic megacolon can lead to additional complications if they become infected with *Shigella* spp. (Phalipon and Sansonetti, 2007).

Worldwide there are more than 164 million cases of shigellosis every year, 99% of which are in developing countries (www.who.int/vaccine_research/disease/shigella/en/). More than one million of these 164 million cases result in death (www.who.int/vaccine_research/disease/shigella/en/). Children under five are at the highest risk of fatality because of complications resulting from malnutrition

and dehydration, accounting for 61% of all deaths from shigellosis and 69% of the total number of *Shigella flexneri* infections (www.who.int/vaccine_research/disease/shigella/en/). *S. flexneri* is found most commonly in underdeveloped countries while *S. sonnei* is usually found in developed countries (Niyogi, 2005). *S. dysenteriae* outbreaks can be found in both (Niyogi, 2005). The fourth species, *S. boydii*, is rarely found outside the Indian subcontinent (Niyogi, 2005).

Shigella infections are primarily transmitted though the fecal-oral route (DuPont, 1989). With conditions such as contaminated or uncooked food, water supplies contaminated with sewage, poor hygienic practices, and overcrowding contribute to epidemics (DuPont, 1989). Outbreaks that occur in the United States and Europe affect certain groups of people more often than others (Niyogi, 2005). Those at higher risk include children in day-care centers, migrant workers, travelers to developing countries, workers of custodial institutions and homosexual men (Niyogi, 2005). In the United States *S. sonnei* is found three times more often than *S. flexneri* but *S. flexneri* is the species usually found in infected homosexual men (Niyogi, 2005). When associated with human immunodeficiency virus (HIV) or acquired immune deficiency syndrome (AIDS), *S. flexneri* can lead to complications including persistent or recurrent intestinal disease and bacteremia (Niyogi, 2005). *S. flexneri* is commonly associated with these infections in developing countries, while epidemic outbreaks are usually attributed to *S. dysenteriae*. Most fatal cases of shigellosis are the result of infection by *S. dysenteriae* and the production of an efficacious exotoxin (Shiga

toxin) (O'Brien *et al.*, 1980). It is a potent cytotoxin responsible for intestinal symptomatology and other major systemic complications, including Hemolytic Uremic Sydnrome (HUS) (Phalipon *et al.*, 2008).

Shigella flexneri enters a host orally, making its way to the large intestine where it invades the colonic epithelium after passing through the upper digestive system. The bacterium easily survives passing through the upper digestive tract and small intestine into the colon due to its high acid tolerance (Sur, 2004). It has been shown that *Shigella* spp. are able to promote their own invasion of the colonic epithelium by down regulating certain antimicrobial peptides that are released in the gastrointestinal tract, thereby decreasing the host's innate immune response (Islam *et al.*, 2001). During invasion of the intestinal epithelium, *Shigella* spp. must reach the basolateral side of the epithelial cell before they can initiate cell invasion, as they are unable to infect via the apical face (Schroeder and Hilbi, 2008). Once in the large intestine, microfold cells (M cells) in the colon ingest *S. flexneri* in vacuoles via macropinocytosis (Niyogi, 2005) (Owen, 1986). It then escapes the vacuole into the cytosol, traveling to macrophages associated with M cell-associated lymphoid follicles (Sansonetti *et al.*, 1996). *S. flexneri* is exposed to the resident macrophage, whose job it is to engulf and degrade any incoming material, after being transcytosed into an intraepithelial pocket by M cells (Schroeder and Hilbi, 2008).

After transcytosis to the intraepithelial pocket and engulfment by macrophages, *S.flexneri* begins initiating apoptosis of those macrophages, via a caspase1-dependent pathway, leading to release of the proinflammatory

cytokines interleukin-1β (IL-1β) and IL-18 (Schroeder and Hilbi, 2008) (Sansonetti, 2000). IL-1β is responsible for triggering the major inflammation shigellosis causes in the lower intestine; however both cytokines activate acute and inflammatory responses (Schroeder and Hilbi, 2008) (Sansonetti, 2000). IL-18's role is not fully understood but it is known that it increases the innate immune response by activating natural killer cells and promoting gamma interferon production (Schroeder and Hilbi, 2008) (Sansonetti, 2000). The inflammation caused by the infection leads to recruitment of IL-8, which then recruits polymorphonuclear leukocytes (PMN) that allow more bacteria to bypass the M cells to reach the submucosa via destabilization of the epithelial lining (Schroeder and Hilbi, 2008) (Sansonetti, 2000). *S. flexneri* also alters the protein composition of the tight junctions of epithelial cells to loosen them (Schroeder and Hilbi, 2008). This combination of effects initially facilitates the invasion, causing the bloody diarrhea *S. flexneri* is well known for, until the immune system takes over and begins killing the bacteria (Schroeder and Hilbi, 2008).

After crossing the epithelial barrier of the colon, *S. flexneri* can then induce its own ingestion by the colonic epithelial cells and it can begin using actin based motility (ABM) to move through the cytoplasm to promote entry into neighboring epithelial cells laterally (Mounier *et al.*, 1992). This further contributes to the inflammatory process. Ultimately, the symptoms attributed to shigellosis, inflammation and ulceration of the mucosa in the colon, however, are the result of the response to infection by the host's immune system (Wassef *et al.*, 1989) (Islam *et al.*, 1997).

Invasion via the Basolateral Face

After killing subepithelial macrophages, shigellae invade colonic epithelial cells from their basolateral face (Sansonetti *et al.*, 1986). Once inside these cells, shigellae must escape from the phagosome into the cytoplasm before they can begin replicating and spreading to adjacent colonic epithelial cells (Sansonetti *et al.*, 1986). It was shown that the loss of the 31-kb entry region in *S. flexneri* strains leads to the loss of invasiveness and the ability to escape the phagosome. These functions can be restored by complementation with the *Sallmonella enteric* serovar Typhimurium *Sallmonella* pathogencity island-1 (SPI-1) (Paetzold *et al.*, 2007). Due to the homology of the genes contained in SPI-1 to the genes on the large virulence plasmid of *S. flexneri*, complementation is not surprising (Paetzold *et al.*, 2007). One major difference between these two bacteria (*S. typhimurium* and *S. flexneri*) is that the former can replicate inside the phagosome while the latter must escape before it can begin replication (Tekouchi, 1967) (Sansonetti *et al.*, 1986). Complimentation by SPI-1 returns the ability to invade and escape the phagosome, even if the 31-kb region is missing (Paetzold *et al.*, 2007). If the entire plasmid is missing, complementation with SPI-1 only allows *S. flexneri* to invade a host cell, but does not restore the ability to escape the phagosome (Paetzold *et al.*, 2007). This suggests that the genes required for *S. flexneri* to escape the phagosome are contained on the virulence plasmid but not in the 31-kb entry region (Paetzold *et al.*, 2007).

To induce cytoskeletal rearrangement and phagocytosis into the host cell, additional TTSS effectors are secreted by *Shigella* spp. after the formation and insertion of a "translocon pore" into the host cell's cytoplasmic membrane (Menard *et al.*, 1994) (Watarai *et al.*, 1995) (Menard *et al.*, 1996) (Blocker *et al.*, 1999). The pathways by which these interactions occur are not fully understood. There are five effector proteins most commonly studied with regard to the induction of phagocytosis by the host cell, IpaA, IpgB1, IpgB2, IpaC and IpgD. IpaA is able to depolymerize actin, and IpgB1 and IpgB2 are able to induce membrane ruffling by mimicking RhoG and RhoA, respectively (Alto *et al.*, 2006) (Handa *et al*., 2007). IpaC has been proposed to interact with Cdc42 and to nucleate actin (Terry *et al.*, 2008) (Tran Van Nhieu *et al.*, 1999). The last of the commonly studied effectors is IpgD which is described as a phosphoinositide 4-phosphate that has the ability to hydrolyze phosphatidylinositol-4,5-biphosphate [PtdIna(4,5)P_2], thereby disassociating the cytoskeleton from the plasma membrane (Hilbi, 2006) (Niebuhr *et al.*, 2002).

After *S. flexneri* escapes the phagosome, it can begin its lateral spread through the colonic epithelium. While *S. flexneri* is a non-motile bacterium, it can use actin-based motility to move within the cytoplasm of the host cell. The actin polymerization is controlled by IcsA (intracellular spread) which localizes to the old pole after cell division (Purdy, 2007). IcsA (also know as VirG) is able to interact with host cell N-WASP and Arp^2/Arp^3, with the help of IcsP and PhoN2, which allows the nucleation of actin and movement throughout the cytoplasm (Purdy, 2007). To make a path for *S. flexneri* movement, another protein, VirA,

works at the opposite pole to depolymerize α-tubulin, allowing the bacterium to pass through the host cell's thick intracellular microtubular network (Yoshida *et al.*, 2006).

The goal of *Shigella flexneri* is to enter a cell, replicate, then enter another cell, replicate, and so on, continuing its lateral spread throughout the colonic epithelium. *S. flexneri* needs to reach the host cell cytoplasm to replicate and to protect itself from the extracellular immune system components (Schroeder and Hilbi, 2008). The replicative niche of *S. flexneri* is the cytoplasm of epithelial cells (Schroeder and Hilbi, 2008). Once it escapes the vacuole into the cytoplasm it must protect itself from intracellular defense autophagy using IcsB to mask IcsA, which contains an autophagy-inducing recognition site (Schroeder and Hilbi, 2008). Using actin based motility, *S. flexneri* moves to the tight junctions between the host epithelial cells where it can be taken up by the adjoining epithelial cell where it resides inside of a double-membrane vacuole (Schroeder and Hilbi, 2008). It then escapes into the new cell's cytoplasm by lysing the vacuole using the TTSS to secrete various effectors. It then begins the process of replication and further lateral spread through the colonic epithelium (Figures 1.1 and 1.2).

Pathogenic Shigellae

Shigella spp. belong to the family Enterobacteriaceae and are closely related to members of the genus *Escherichia* (Kreig and Holt, 1984). Shigellae

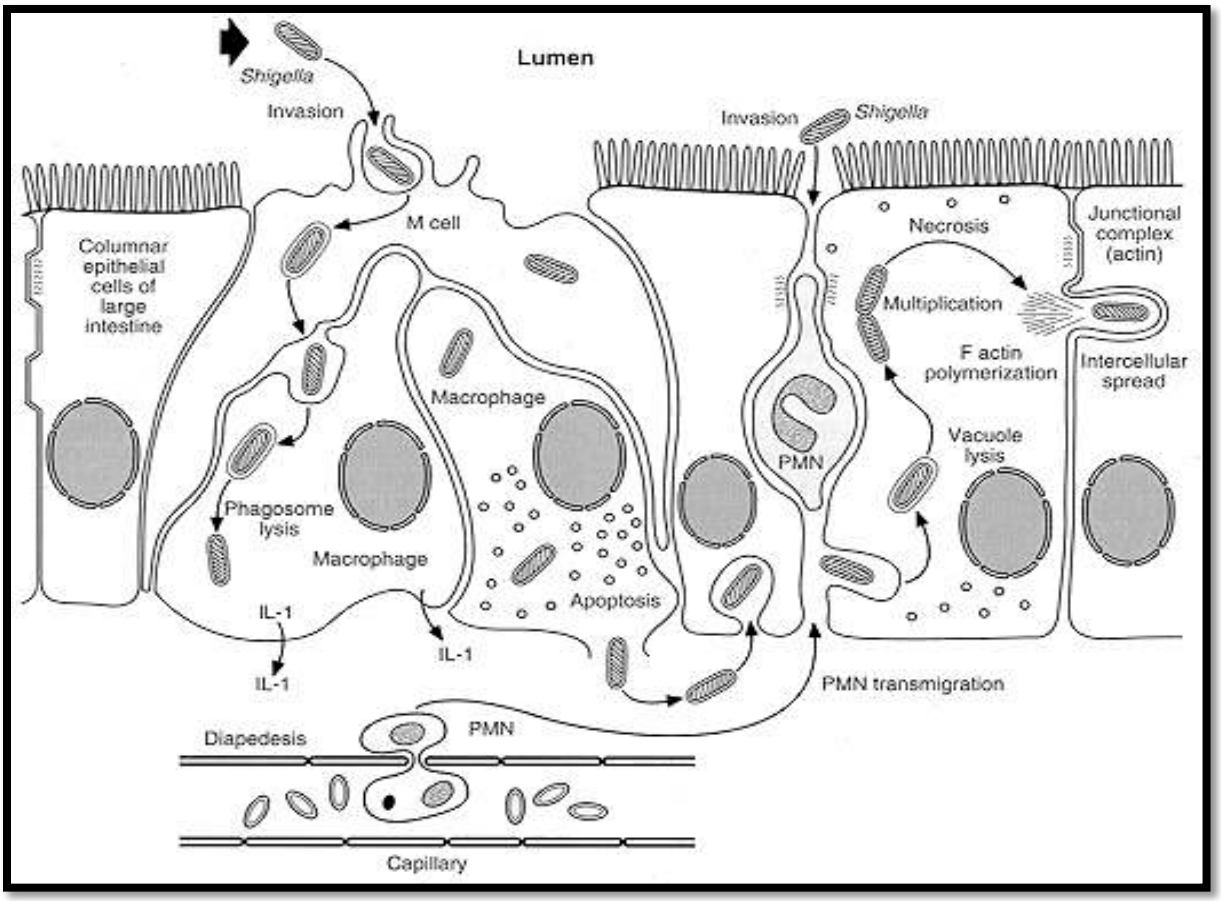

Figure 1.1 Schematic of *Shigella flexneri* Infection
Shigella flexneri is ingested by the M cells of the colon, exposed to the resident macrophages inducing their apoptosis, then moves through the cell to the basal face. It then uses the TTSS to induce its own uptake into the cell where it can escape the vacuole into the cytoplasm. Once in the cytoplasm it can replicate and use propulsion from actin polymerization to spread to adjacent epithelial cells. (http://www.utmb.edu/gsbs/microbook/ch022.htm)

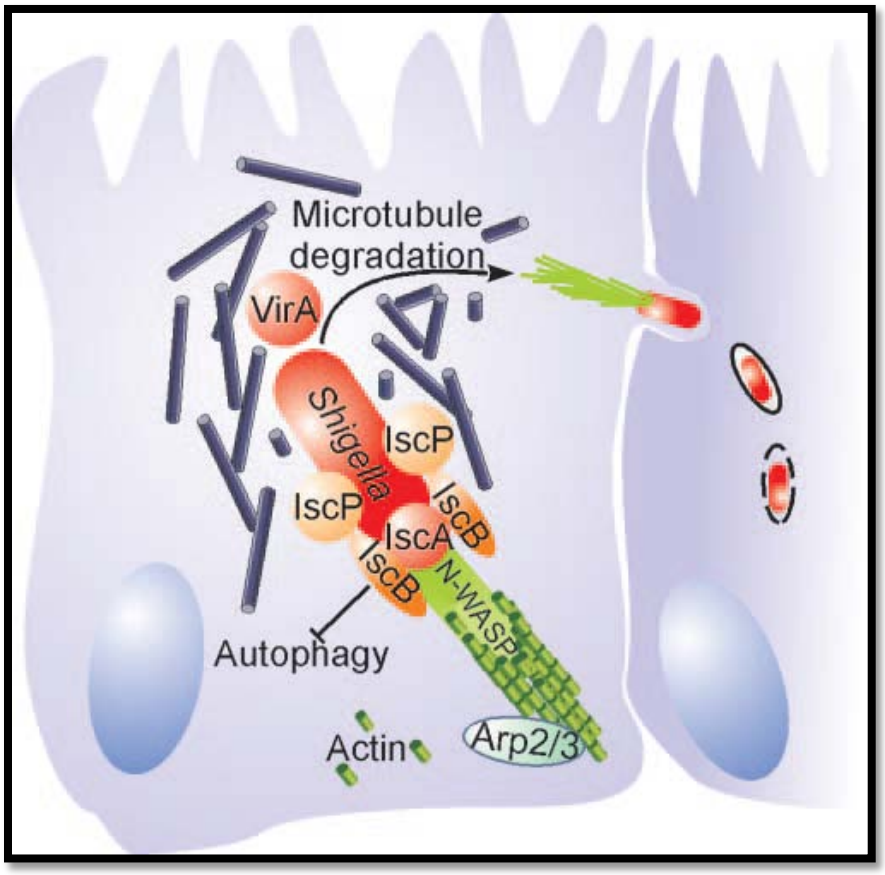

Figure 1.2 Intracellular Movement of *Shigella flexneri*
Shigella flexneri utilizes IcsA to form an actin tail allowing it to move throughout the cytoplasm and VirA to degrade microtubules allowing the bacteria to penetrate the adjoining epithelial cell. (Schroeder and Hilbi, 2008)

are gram-negative gastrointestinal pathogens that cause disease in humans and higher primates, as do the other pathogens in its family including *Salmonella*, *Yersina*, and *Escherichia* (DuPont *et al.,* 1989). Similar to its family members, these bacteria are facultatively anaerobic, oxidase negative, and they have the ability to reduce nitrate and ferment glucose (Kreig and Holt, 1984). Testing for ornithine decarboxylation and manitol and xylose fermentation allows for biochemical differentiation between the species (Kreig and Holt, 1984). Also, the species can be differentiated serologically based on the species-specific O-antigen components that each contains (Kreig and Holt, 1984). There are four serotypes A, B, C and D belonging to the four species *S. dysenteriae, S. flexneri*, *S. boydii* and *S. sonnei,* respectively (Niyogi, 2005).

Shigella spp. require very few organisms, approximately 10-100, to elicit the disease shigellosis, making it extremely infectious and easily spread (DuPont e*t al.*, 1989). Poor sanitation and contaminated food or water sources are usually the cause of outbreaks of shigellosis. Infected people who display the symptom of diarrhea are most responsible for transmission of the disease (Niyogi, 2005). Shigellosis is usually self-limiting with symptoms lasting five to seven days and it can be treated orally with antibiotics (Hueck, 1998). However, infected patients can spread the disease as long as they are excreting the organism which can last up to four weeks (Sur, 2004). This length of time can be reduced if properly treated with antibiotics (Sur, 2004).

Today, treatment consists mainly of oral antibiotics, including quinolones, levofloxacin or norfloxacin and the macrolide azithromycin, but the number of

effective antibiotics available for use is constantly decreasing due to the emergence of new antibiotic resistant strains (Niyogi, 2005). Worldwide, strains of shigellae have emerged that are resistant to many antibiotics including tetracycline, sulfonamides, ampicillin and trimethoprim-sulfamethoxazole (Hueck, 1998). To avoid dehydration, an infected person should consume electrolyte drinks to replace fluids and restore nutrients lost from diarrhea during treatment for shigellosis along with proper antibiotic treatment for the disease (http://www.nlm.nih.gov/medlineplus/ency/article/000295.htm).

Genetics of Virulence

All *Shigella* spp. contain a large virulence plasmid. The genes it encodes, along with the genes encoded on the pathogenicity islands located in its chromosome, are the basis for shigellae virulence (Schroeder and Hilbi, 2008). Virulence factors including antibiotic resistance, iron acquisition and proteases can be found encoded on the pathogenicity islands (Schroeder and Hilbi, 2008). All the genes for cellular invasion are contained on the large virulence plasmid, the most important aspect of shigellae virulence. This large plasmid is about 200-kb with approximately 100 genes, but it can vary in size among the four species (Maurelli *et al.*, 1985) (Yoshikawa *et al.*, 1988). The virulence plasmid contains genes necessary for the uptake by epithelial cells and dissemination of the bacteria throughout the colonic epithelium (Wantanabe, 1990). The entry region of the virulence plasmid, 31-kb in size, encodes a type III secretion system (TTSS) that facilitates cellular uptake (Schroeder and Hilbi, 2008). The plasmid

contains other genes that encode proteins used after invasion of a host cell (Sansonetti, 1982) (Yoshikawa *et al.*, 1988). Contained in the 31-kb entry region are the *mxi-spa* operon and *ipa-ipg* operon which are responsible for encoding the type III secretion apparatus (TTSA) and the type III secreted protein effectors/translocators IpaA, IpaB, IpaC, IpaD and the molecular chaperone IpgC (Espina *et al.*, 2006). Research has shown that if shigellae lose this large plasmid they cannot infect and cause disease (Yoshikawa *et al.*, 1988). It has also been shown that non-pathogenic lab strains of *E. coli* can become invasive after receiving the *Shigella* virulence plasmid (Sansonetti, 1982).

The genes in the entry region can be differentiated into four categories based upon their specific functions (Schroeder and Hilbi, 2008). Proteins secreted by the TTSA comprise the first category. They are mainly the *ipa* (invasion plasmid antigen) genes, whose functions are generally considered to be as effector and/or translocator proteins that are directly involved in the induction of cytoskeletal rearrangement, cell membrane ruffling and pathogen uptake (macropinocytosis) (Espina *et al.*, 2007) (Schroeder and Hilbi, 2008). The second group is composed of the TTSA structural genes. They are the *mxi* (membrane expression of ipa proteins) and *spa* (surface presentation of ipa antigens) genes (Espina *et al.*, 2007) (Schroeder and Hilbi, 2008). The TTSS apparatus consists of a basal body and needle that are composed of various polymers of the Mxi and Spa structural proteins (Espina *et al.*, 2007). Expression of the early and late entry region genes are controlled by different transcriptional activators, MxiE and VirB for example, which make up a third group of key TTSS

components (Schroeder and Hilbi, 2008). The last group consists of the molecular chaperones, whose function is to maintain effector and translocator proteins while they are stored in the bacterial cytoplasm prior to secretion (Schroeder and Hilbi, 2008).

Bacterial Secretion Systems

All bacteria possess secretion systems as part of their normal function. In addition many gram-negative bacterial pathogens use dedicated secretion systems to transport effector molecules or virulence factors into their environment or into targeted host cells as a key part of their virulence. Currently, there are six named bacterial secretion systems which have been classified based on the numbering system I, II, III, IV, V and VI. Two of the systems are *sec*-dependent (secretory), types II and V, while types I, III and IV are classified as being *sec*-independent (Russel, 1998) (Harper and Silhavy, 2001). The two *sec*-dependent secretion systems make use of the machinery of the general secretory pathway to translocate proteins across the inner membrane of bacteria (Russel, 1998) (Harper and Silhavy, 2001). They do this by catalyzing and translocating the proteins across the bacterium's inner membrane to its periplasmic space via as N-terminal signal peptide that is removed in the process (Russel, 1998) (Harper and Silhavy, 2001). The type VI secretion systems are relatively new, being discovered in 2006 in *Vibrio cholerae* by Stefan Pukatzki *et al* (Pukatzki *et al.*, 2006). It has since been found in several gram-negative bacteria including *Psedomonas aeurginosa* and *Burkholderia cenocepacia*,

however, this system is not yet very well characterized (Aubert *et al.*, 2008) (Zheng and Lewis, 2007) (Pukatzki *et al.*, 2006). It is thought to be *sec*-independent due to the absence of an N-terminal signal sequence on the proteins that are secreted (Pukatzki *et al.*, 2006).

Type I secretion systems are the simplest of the six, containing only three proteins an ABC protein or ATP binding cassette protein, a membrane fusion protein and an outer membrane trimeric protein. Type I secretion systems transport proteins in a single step through a continuous channel from the inner membrane, through the periplasm, to the outer membrane (Holland *et al.*, 2005). Type II secretion systems utilize the *sec* pathway to transport proteins to the periplasm where it then uses a complex of 12-14 protein components to transport the proteins from the periplasm to the environment surrounding the cell (Russel, 1998). The type III secretion system (already described in part) is made up of a basal body that spans the inner and outer membranes and an extracellular needle complex which allows the bacteria to directly inject effectors directly into a target cell's cytoplasm. Type III secretion is an ATPase-driven system and it has been termed contact dependent secretion since contact with a host cell is the typical signal needed to induce this secretion (Hueck, 1998). Type IV secretion systems were originally thought to be limited to conjugal transfer systems that transport bacterial DNA between bacteria to facilitate natural genetic exchange (Winans *et al.*, 1996). It has since been determined that this pilus-like transport system can also export monomeric and multisubunit proteins, as well as bacterial DNA, into eukaryotic cells (Winans *et al.*, 1996). There are three kinds of type IV

secretion systems: 1) conjugation systems; 2) effector translocator systems; and 3) DNA release/uptake systems (Alvarez-Martinez and Christie, 2009). The first two of which usually require direct contact with a target cell for activation (Alvarez-Martinez and Christie, 2009). Type V secretion systems are known as autotransporters or two-partner secretion systems (Jacob-Dubuisson *et al.*, 2004) They utilize the *sec* pathway for the first step in their function (Jacob-Dubuisson *et al.*, 2004). Type V secretion systems export large proteins possessing an N-terminal *sec*-dependent signal domain, the mature portion of the protein, and a C-terminal translocation unit that contains three regions, α-, β- and γ- (Jacob-Dubuisson *et al.*, 2004) (Klauser *et al.*, 1993). The *sec* signal domain allows the protein to move through the inner membrane and into the periplasm via the standard *sec* pathway machinery (Jacob-Dubuisson *et al.*, 2004) (Klauser *et al.*, 1993). The β-region then inserts itself into the bacterium's outer membrane where it forms a pore that has characteristic β-barrel structure (Klauser *et al.*, 1993). This pore allows the passage of the remaining regions (often referred to as the "cargo" regions) through the outer membrane where they can be cleaved by autoproteolysis and released into the extracellular environment (Klauser *et al.*, 1993). In some cases the cargo remains attached as a bacterial surface protein (Klauser *et al.*, 1993). The type V system is not as versatile as the other secretion systems, such as the type II or type III systems, due to its ability to only secrete one molecule of the natural extracellular protein substrate (Jacob-Dubuisson *et al.*, 2004). Type VI secretion systems are the least characterized and understood with little known about their structure and mechanism. It has

been found in several gram-negative bacteria in addition to the ones previously listed (Aubert *et al.*, 2008) (Zheng and Leung, 2007) (Pukatzki *et al.*, 2006).

The Type III Secretion System

In order to invade the epithelial cells of the human colon, *Shigella* spp. utilize the TTSS and a set of secreted translocator and effector proteins for targeting, penetrating and generally manipulating a host cell. The TTSA is able to directly inject effector proteins into a host cell's cytoplasm, thereby acting as a molecular syringe. After injection of effectors, cytoskeletal rearrangements and ultimately uptake of the bacterium are mediated by the interaction of the effector proteins and their target signaling molecules within the host cell (Cornelis, 2006).

The TTSA is composed of a basal body that spans the inner and outer membrane of the bacterium, and an extracellular needle protruding from the bacterium's outer membrane into the surrounding environment (Schroeder and Hilbi, 2008). The basal body structure is composed of seven rings, while the needle is a MxiH polymer approximately 50 nm long, 7 nm wide with an inner channel that has a diameter of about 2.5 nm (Epler *et al.*, 2009). On the cytoplasmic face of the bacterium, the TTSA possesses an ATPase that has been shown to be involved in protein unfolding, chaperone release and transmembrane transport of substrate proteins (Figure 1.3) (Blocker *et al.*, 2001).

The Ipa Proteins

To gain entry into a target cell and take control of the cytoskeletal proteins needed to promote bacterial uptake, *Shigella* utilizes several secreted effector proteins. At the tip of the MxiH polymer needle is IpaD, which is believed to participate in sensing environmental signals and initiating the process of secretion induction (Espina *et al.*, 2006). IpaD is also a major secretion substrate in *Shigella* type III secretion. IpaD sensing of bile salts in the intestine leads to IpaB secretion and recruitment to the TTSA needle tip (Stensrud *et al.*, 2008). At this point, the *Shigella* TTSS is prepared for full induction of type III secretion. After subsequent contact with a host cell, the *Shigella* TTSS then begins the secretion of other effectors that include the final translocator protein IpaC and additional effectors that are secreted into the host cell cytoplasm (Epler *et al.*, 2009) (van der Goot *et al.*, 2004). Several labs have shown that conditions mimicking host cell contact can induce secretion by the TTSA. The addition of small amphipathic dyes, such as Congo red, brilliant orange or Evens blue, appear to mimic host cell contact to induce *Shigella* type III secretion (Parsot *et al.*, 1995) (Bahrani *et al.*, 1997).

Espina *et al.* demonstrated that IpaD localizes to the tip and caps the MxiH polymer needle of the TTSA (Espina *et al.*, 2006). The inability of IpaD null mutants to invade and their hypersecretion of TTSS effectors into the extracellular environment during overnight cultures demonstrate IpaD serves as a crucial component of the *Shigella* TTSS, perhaps as a regulatory component controlling type III secretion (Menard *et al.*, 1994) (Picking *et al.*, 2005). Work

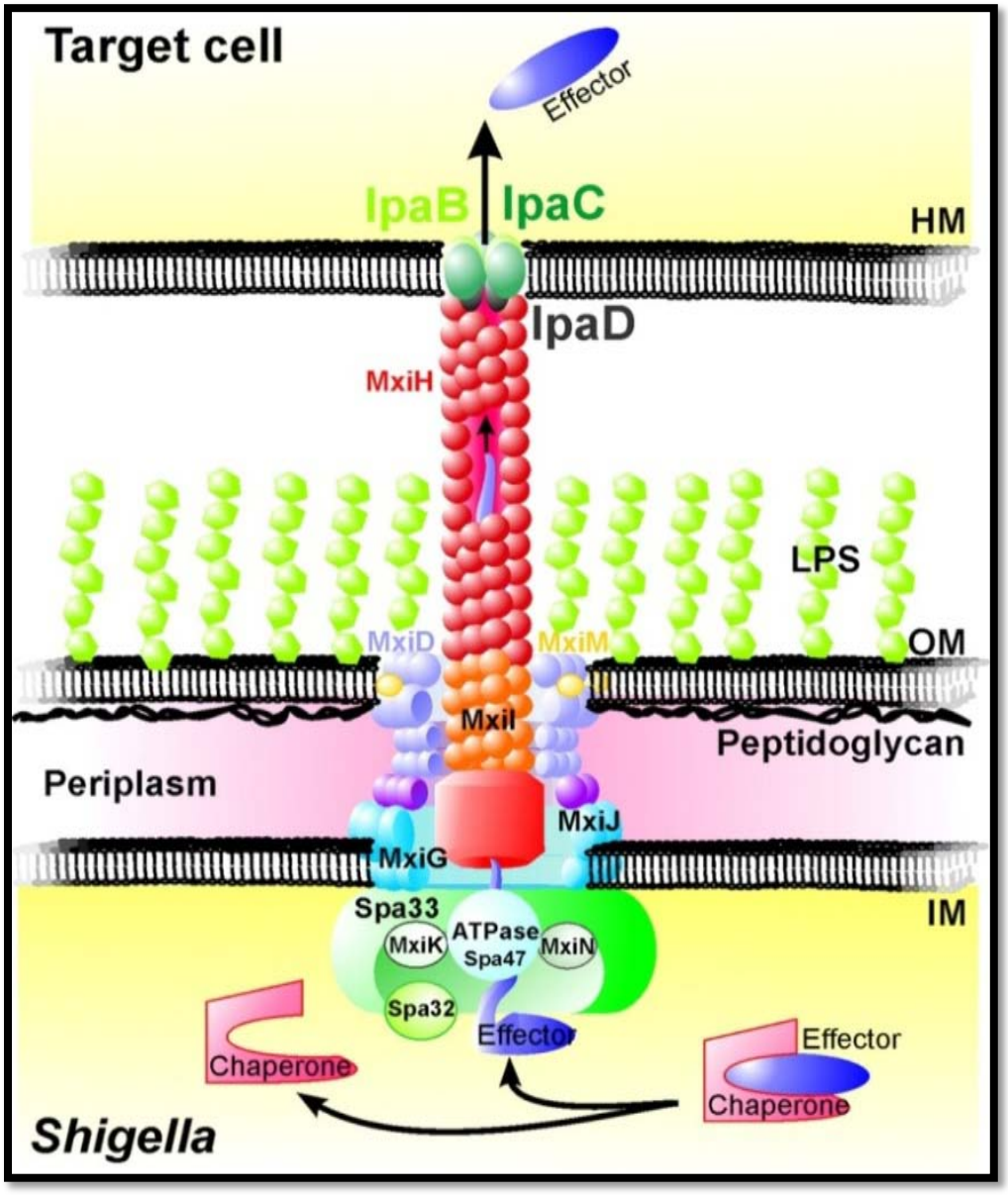

Figure 1.3 The Type III Secretion System (TTSS) of *Shigella flexneri*
The TTSS of *S. flexneri* with the membrane spanning basal body and extracellular needle protruding from the surface. This shows the TTSS in contact with a host cell and the tip complex assembled along with the translocon inserted into the host cell membrane (Schroeder and Hilbi, 2008).

done by our group has shown that secretion of IpaB can be induced by the presence of bile salts, specifically deoxycholate, which leads to IpaB colocalizing with IpaD at the distal tip of the needle (Olive *et al.*, 2007). IpaB possesses a cholesterol binding function that may serve as a priming step that allows the needle to recognize bacterial interaction with the host cell (Hayward *et al.*, 2005).

Within the cytoplasm of *S. flexneri*, *the* molecular chaperone IpgC (invasion plasmid gene) binds to IpaB before it is secreted (Birket *et al.*, 2007). IpgC prevents the aggregation of IpaB in the bacterial cytoplasm and its association with the other translocator protein IpaC (Menard *et al.*, 1994) (Page *et al.*, 1999) (Lunelli *et al.*, 2009). IpaB binding to IpgC is also thought to stabilize IpaB in a pre-secretion state prior to its passage through the TTSA needle (Menard *et al.*, 1994) (Page *et al.*, 1999). It was shown by circular dichroism (CD) spectroscopy that IpgC has a significant α-helical secondary structure (data not shown). This has been confirmed by the solving of IpgC's crystal structure (Lunelli *et al.*, 2009). IpaB and IpaC are less ordered (based on CD analysis), but the binding of IpgC to IpaC induces significant secondary structural change, increasing the amount of α-helical structure, and stabilization (Birket *et al.*, 2007). IpgC is believed to have a similar effect on IpaB, but the details of this, such as the specific residues or regions involved, have not been determined (Birket *et al.*, 2007).

IpaB is important to study because it has several functions that are key to *Shigella* pathogenesis. As a secreted effector protein, as a regulator of type III secretion and as a structural protein in the formation of the *Shigella* translocon

pore that forms in the host cell membrane (Schroeder and Hilbi, 2008). To escape the macrophage after initially crossing M cells, *S. flexneri* secretes IpaB to induce apoptosis via a caspase1-dependent pathway (Hilbi, 1998). This apoptotic (pyroptotic) pathway results in the massive release of IL-1β, which provides the signal for induction of the inflammatory process that give rise to the symptoms of shigellosis (Sansonetti, 2000). IpaB also serves to control effector regulation, as does IpaD (Menard *et al.*, 1994). *IpaB* null mutants show the same overall phenotype as do *ipaD* null mutants, including non-invasiveness and *hyper*secretion of effectors into the extracellular supernatant of overnight cultures (Menard *et al.*, 1994). IpaB is also one component of the two-part translocon pore that becomes inserted into the host cell's cytoplasmic membrane shortly after host cell contact. The other translocon component is IpaC (Schroeder and Hilbi, 2008). IpaD allows this pore to remain in contact with the TTSA needle tip (Schroeder and Hilbi, 2008). This pore allows formation of a channel through the membrane to the host cell's cytoplasm, thereby allowing direct injection and secretion of later effectors directly from the bacterial cytoplasm to the host cell's cytoplasm (Menard *et al.*, 1994) (Zychlinsky *et al.*, 1994) (Blocker *et al.*, 1999).

Along with IpaB, the IpgC chaperone binds to the second translocator/effector protein, IpaC, keeping it stable in the cytoplasm until it joins IpaB as a translocon pore component (Menard *et al.*, 1994) (Page *et al.*, 1999). Along with forming the translocon pore, IpaC is also involved in signaling to the host cell. Cdc42 is a small Rho-family GTPase that IpaC has been proposed to interact with to induce formation of filopodial extensions (Tran Van Nhieu *et al.*,

1999). Little is known about this interaction, but it has been shown that IpaC can nucleate actin (Kueltzo *et al.*, 2003). Recent findings suggest that the ability for IpaC to nucleate actin is much more important than its ability to interact with Cdc42 (Terry *et al.*, 2008).

The Molecular Chaperone IpgC

Invasion plasmid gene C (IpgC) is the molecular chaperone for IpaB and IpaC, both of which are translocator proteins for the *Shigella* TTSS (Parsot *et al.*, 2003) (Birket *et al.*, 2007). There are three classes of molecular chaperones used by the TTSS (Parsot *et al.*, 2003) (Birket *et al.*, 2007). Class I chaperones are associated with late effector proteins that are targeted for direct injection into the target cell's cytoplasm (Parsot *et al.*, 2003). These can be divided into two subclasses, IA and IB, depending on whether they bind with one protein, IA, or more than one protein, IB (Parsot *et al.*, 2003) (Birket *et al.*, 2007). The class II chaperones associate with the translocator proteins for its cognate TTSS (Parsot *et al.*, 2003) (Birket *et al.*, 2007). The class III chaperones bind with proteins of the flagellar TTSS and these are not relevant in *Shigella* (Parsot *et al.*, 2003) (Birket *et al.*, 2007). Several defining characteristics are common of most TTSS chaperones. They are their small molecular masses and low *p*Is (Parsot *et al.*, 2003) (Birket *et al.*, 2007). Some chaperones are also responsible for regulating late gene expression by interacting with transcription factors after initial contact with the host cell (Parsot *et al.*, 2004). IpgC is a class II molecular chaperone specific for IpaB and IpaC, all of which are encoded on the *ipa/ipg* operon of

Shigella flexneri (Birket *et al.*, 2007). IpgC is responsible for complexing with and stabilizing the translocators IpaB and IpaC within the bacterial cytoplasm, thus preventing their interaction and/or degradation until type III secretion is activated (Birket *et al.*, 2007). IpgC is a small (20 kDa) protein with a very acidic *p*I of 4.6, which is responsible for several roles including acting as a chaperone and acting as a transcription activator within the Shigella TTSS after association with MxiE (Cornelis and Van Gijsegem, 2000) (Page *et al.*, 2001) (Birket *et al.*, 2007).

IpgC serves as a transcriptional co-activator of *virA* and *ipaH9.8* (Pilonieta and Munson, 2008). Pilonieta and Munson showed that production of VirA and IpaH9.8 can be increased when IpgC and MxiE associate which was determined trough co-purification experiments (Pilonieta and Munson, 2008). While originally thought to be a transient interaction, Pilonieta and Munson showed that the increased transcription of *virA* and *ipaH9.8* is only seen after the release of IpgC from both IpaB and IpaC (Pilonieta and Munson, 2008).

IpgC's interaction with IpaB and IpaC is of interest due to its ability to bind multiple partners having little or no sequence similarity (Birket *et al.*, 2007). IpgC's effect on IpaC has been investigated by other members of the lab to better understand IpaC's function as a *Shigella* virulence determinant and IpaC's role in this process. IpaC is a 42 kDa protein with functions that include the ability to disrupt liposomes, interact with actin, and to promote invasion of epithelial cells (Picking *et al.*, 2001) (Kueltzo *et al.*, 2003). It has been shown that IpgC's binding with IpaC induces significant conformational changes within

the latter protein while simultaneously stabilizing IpaC's secondary structure (Birket *et al.*, 2007). No such data are available for the IpgC/IpaB interaction.

Research Focus

The research presented here is intended to further our understanding of the structure and topography of IpaB, in the presence and absence of binding to its chaperone IpgC. Structural information of IpaB is limited due to its large size, (62 kDa) and hydrophobicity, however, several key regions of IpaB have been determined based on the predicted secondary structure analysis and structure-function analyses from mutagenesis studies (Birket *et al*., 2007). This study is intended to further past structure analyses and to better understand and characterize key regions within IpaB and its structure by generating the first biophysical and structural data available for this protein. I hypothesize that IpaB is a highly structured protein, with and without its IpgC chaperone, and is more thermally stable when bound to IpgC which will be tested using a variety of spectroscopic analyses. These findings will be extended using tryptophan scanning mutagenesis to help determine the topology of IpaB, which will perhaps allow identification of regions involved in IpaB's interaction with IpgC.

Within the cytoplasm of *Shigella flexneri*, IpaB is complexed with IpgC until it disassociates to become loaded into the needle for export to the TTSA neddle tip. This is why it is important to study the influence IpgC's binding has on IpaB's structure. IpaB has two key roles, inducing apoptosis in the macrophage after ingestion and interacting with IpaC to form the translocon pore that is inserted

into the host cell membrane, both of which are vital steps of *S. flexneri* infection. If IpaB is not secreted, *S. flexneri* cannot induce apoptosis to escape the macrophage. Without the IpaBC translocon pore, *S. flexneri* becomes noninvasive and it is incapable of causing disease in a host. Others have studied and characterized the IpaBC translocon pore interactions along with IpaC and IpgC interactions (Birket *et al.*, 2007). Some of the same biophysical and molecular methods utilized in those studies have been applied in this study to better characterize the structure of IpaB, its interactions with IpgC and the conformational changes when associated with other protein partners. I will combine tryptophan scanning mutagenesis with Trp fluorescence analysis, thermal unfolding scans and Förster resonance energy transfer from Trp to a covalently linked extrinsic fluorescent probe.

CHAPTER II

MATERIALS AND METHODS

Reagents and Buffers

Coomassie Blue Protein Gel Stain
250 ml methanol
1.25 g Coomassie brilliant blue
75 ml acetic acid
175 ml diH_2O

8X His-Tag Binding Buffer
2.72 g imidazole
237 g NaCl
19.36 g Tris
Adjust to 1.00 L with diH_20

4X His-Tag Charge Buffer
52.56 g $NiSO_4$
Adjust to 500 ml with diH_2O

4X His-Tag Elution Buffer
136 g imidazole
58.44 g NaCl
4.84 g Tris
Adjust to 500 ml with diH_2O
pH to 7.9

4X His-Tag Strip Buffer
74.4 g EDTA
58.44 g NaCl
4.84 g Tris
Adjust volume to 500 ml with diH_2O
pH to 7.9

8X His-Tag Wash Buffer
5.44 g imidazole
117 g NaCl
9.68 g Tris
Adjust volume to 500 ml with diH_20
pH to 7.9

Luria-Bertani Broth (LB)
25.0 g LB broth
1.00 L diH_2O

Luria-Bertani Agar (LB)
40.0 g LB agar
1.00 L diH_20

10X Phosphate Buffered Saline (PBS)
85.0 g NaCl
10.7 g sodium phosphate, dibasic
3.90 g sodium phosphate, monobasic
1.00 L diH_2O

10% SDS-PAGE Separating Gel
4.00 ml diH_20
2.50 ml 1.5 M Tris-HCL, pH 8.8
100 µl 10% SDS
3.33 ml 30% Bis:Acrylamide

12% SDS-PAGE Separating Gel
3.00 ml diH_20
2.50 ml 1.5 M Tris-HCL, pH 8.8
100 µl 10% SDS
4.00 ml 30% Bis:Acrylamide

15% SDS-PAGE Separating Gel
2.50 ml diH_20
2.50 ml 1.5 M Tris-HCL, pH 8.8
100 µl 10% SDS
5.00 ml 30% Bis:Acrylamide

5% SDS-PAGE Stacking Gel (2)
2.85 ml diH_2O
1.25 ml 0.5 M Tris-HCl, pH 6.8
50.0 µl 10% SDS
1.00 ml 30% Bis:Acrylamide

SDS-PAGE Running Buffer
2.42 g Tris
14.41 g glycine
10.0 ml SDS
1.00 L diH_2O

1X Sodium Phosphate Dialysis Buffer (NaP buffer)
20 ml .5 M NaP
8.77g NaCl
5 mL OPOE
Adjust to 1 L with 1X PBS

Processes

IpaB Tryptophan Mutant Construction

All tryptophan mutations in *ipaB* were generated using inverse PCR with pHS2-IpaB, encoding IpaB, as the template. Primers were made to possess GAGAGA, a restriction site flanking the codon to be mutated and approximately 18 nucleotides beyond the mutation site. Primers for Trp mutagenesis are listed in Table 2.1. Inverse PCR produced a linear fragment which was subsequently digested with the appropriate restriction endonucleases and intromolecularly ligated. GAGAGA sequences are present at the ends of the fragment to increase the efficiency of restriction digestion. Ligation products were transformed into Nova Blue *E. coil*. Resulting plasmids were purified using the QIAGEN QIAquick™ plasmid purification kit. Purified plasmids were electroporated into the *ipaB* null *Shigella flexneri* strain SF620 and placed onto trypticase soy agar (TSA) plates containing Congo red and ampicillin. Ampicillin resistant, red

Mutant	Primer Name and Sequence
L79W	B88f-GAGAGAGAGGCTAGCTCCCAATGGACGCTTTTAATTGGAAACC
	B89r-GAGAGAGAGGCTAGCATTTAATGACTTTGGTGCTTT
F119W	B90f-GAGAGAGAGCTCGAGTGGTCCGATAAAATTAACAC
	B91r-GAGAGAGAGCTCGAGGTTTTTTTGCTGTCTTG
L133W	B53f-GAGAGAGAGACGCGTGACTATGAAAAACAAATTAATAA
	B54r-GAGAGAGAGACGCGTCCATCCTTCAGTTTCAGATAGAA
D169W	B92f-GAGAGAGAGTGGCCAGAGTCACCAGAAAAG
	B93r-GAGAGAGAGTGGCCAGAGGTTCGATAATCTTGTTTG
F227W	B94f-GAGAGAGAGGCTAGCGCTGAACAGCTATCAAC
	B95r-GAGAGAGAGGCTAGCTGTGTTTGACCATGCAGAAAAAGAGTC TATTT
F275W	B96f-GAGAGAGAGCTTAAGAATGATCTGGCTCTATGGCAGTCTCTC CAAGAATCAA
	B97r-GAGAGAGAGCTTAAGAGATTCTTCATTATTTTTTCCA
Y293W	B110f-GAGAGAGAGTACGTAAAGCAGAAGAACTC
	B99r-GAGAGAGAGTACGTACTTCAGCAGCCCACTCATCAGATTTTC TCTC
F382W	B100f-GAGAGAGAGCTCGAGGGCTTGGGCGTCGATC
	B101r-GAGAGAGAGCTCGAGCATTTTTGTCCATGCATCTGAAAGG AGTTT
I446W	B102f-GAGAGAGAGTGGCCAAAGTTTCTCAAGAATTTT
	B103r-GAGAGAGAGTGGCCAAAGGTCTGTGAGGGTTTTA
F471W	B104f-GAGAGAGAGGCCGGCGATGAAGTAATATCCAAACA
	B105r-GAGAGAGAGGCCGGCTGCACCAAGCCATTTATTTAATCTGGC AACAC
F514W	B106f-GAGAGAGAGGCTAGCGACAAATCTAGCAGACCT
	B107r-GAGAGAGAGGCTAGCGCTGTTCTGCCAAACAGCAGAAGCGA CACT
I553W	B108f-GAGAGAGAGAGATCTATTAGCCTCAATGT
	B109r-GAGAGAGAGAGATCTGCCCATACTTCCTGCAATTGGC

Table 2.1 Table of Primers
This table list the primers used with the ΔW template to create the single Trp insertion mutants.

colonies were chosen for further assays as these contained both the electroporated plasmid and the virulence plasmid based on Congo red selection. Congo red (CR) selection is based on the fact that *Shigella* lacking the virulence plasmid appear as large white colonies on CR-containing TSA plates. Virulence plasmid containing bacteria appear as smaller, red colonies. W105F (ΔW) was constructed to remove the natural tryptophan residue in IpaB. This was used as a template for subsequent mutants, in which a Trp was introduced at novel sites.

Construction/Production of Recombinant Proteins

Mutated *ipaB* was subcloned from pHS2 into pET15b. The resulting mutant IpaB/pET15b constructs were then transformed into Nova Blue *E. coli*. Transformants were screened with T7 promoter and terminator primers. Positive plasmids were then purified using a QIAGEN QIAquick™ plasmid purification kit and then co-transformed with IpgC/pACYC into Tuner (DE3) *E. coli*. To select for bacteria containing both plasmids, transformations were plated on LB plates containing ampicillin and chloramphenicol. Several colonies were selected and frozen as permanent stocks. A loop of the permanent stock was resuspended in 50 ml of LB and grown overnight. The 50 ml culture was then divided evenly between 4 L of LB, each containing 100 µg/ml ampicillin and 25 µg/ml chloramphenicol. Cultures were grown to mid-log phase (OD_{600} = 0.6) and the protein expression was induced using 0.5 M isopropyl-thio-2-D-galactopyranoside (IPTG). Induced cultures were grown for an additional three hours. The bacteria were then collected by centrifugation and resuspended in 40

ml/L of culture, with 1X His-tag binding buffer. The bacterial suspension was frozen at –20°C.

Gentamycin Protection Invasion Assay

Henle 407 cells were seeded on a 24 well tissue culture plate and incubated with minimal essential medium (MEM) with Earle's salts and supplemented with 10% bovine serum in CO_2 at 37°C until semi-confluent. *S. flexneri* strains were grown at 37°C with shaking in 10 ml of TSB to mid-log phase (OD_{600} = 0.6). One µl of the bacterial culture was added to Henle cells in MEM-glucose and centrifuged at 1,000 x g for five minutes to force contact. The plates were incubated for 30 minutes at 37°C in a CO_2 incubator. The cells were then washed with MEM-gentamycin (50 grams/L) with 5% bovine serum and incubated at 37°C in a CO_2 incubator for one hour in MEM-gentamycin to kill any extracellular *S. flexneri*. After incubation, the MEM-gentamycin was removed by aspiration, cells were washed once with MEM-glucose no serum, and overlaid with melted agarose in deionized water. They were then overlaid with melted 2X LB agar. Once the agar solidified, cells were incubated at 37°C overnight. Colonies were then counted and invasion was calculated relative to complimented *S. flexneri* strains.

Contact-Mediated Hemolysis

S. flexneri strains were grown to mid-log phase at 37°C with shaking in 10 ml of TSB. Bacteria were collected by centrifugation at 3,200 x g. Bacteria were

resuspended in 200 µl of 1X PBS. Sheep erythrocytes were washed at room temperature with 1X PBS and resuspended in 1X PBS to the original cell concentration. Fifty µl of red blood cells (RBCs) were aliquoted into a 96 well microtiter plate to which 50 µl of the bacterial cell suspension was added per well. Contact was induced by centrifugation at 2500 x g at 22°C for 10 minutes. Microtiter plates were then incubated at 37°C for 1 hour. After incubation, RBC/bacterial pellets were vigorously resuspended in ice cold 1X PBS and centrifuged at 2,500 x g for 15 minutes at 4°C. Supernatants were transferred to clean, empty wells. Hemoglobin release was measured by monitoring absorbance at 545 nm on a µQuant™ microtiter plate reader.

Ni+ Affinity Protein Purification of His-Tag Containing Proteins

Frozen bacterial suspensions were thawed, sonicated and clarified by centrifugation for 15 minutes at 10,000 x g. Three ml of resin were washed with five column volumes (CV) of distilled water. The resin was charged with three CV of 1X His-tag charge buffer and then five CV of 1X His-tag binding buffer. Clarified supernatants were applied to the column, which was washed with an additional five CV of binding buffer. Non-specifically bound proteins were removed with five CV of 1X His-tag wash buffer and bound proteins were then eluted in three CV of 1X His-tag elution buffer. Fractions were collected and analyzed by sodium dodecyl sulfate-polyacrylamide gel electrophoresis (SDS-PAGE) gel to check for protein production. The resin was stripped with three CV of 1X His-tag strip buffer and stored at 4°C.

Ni+ Affinity Protein Purification of His-Tag Containing Proteins with OPOE

Frozen bacterial suspensions were thawed, sonicated and clarified by centrifugation for 15 minutes at 10,000 x g. Three ml of resin were washed with five CV of distilled water. The resin was charged with three CV of 1X His-tag charge buffer and then five CV of 1X His-tag binding buffer. Clarified supernatants were applied to the column; three ml of binding buffer plus 1% n-octyl-poly-oxyethlene (OPOE) was added. The column was allowed to rock overnight in a cold room at 4°C. Non-specifically bound proteins were removed with five CV of 1X His-tag wash buffer with 1% OPOE and bound proteins were then eluted in three CV of 1X His-tag elution buffer with 1% OPOE. Fractions were collected and analyzed by SDS-PAGE gel to check for protein production. The resin was stripped with three CV of 1X His-tag strip buffer and stored at 4°C for future use.

Dialysis of IpaB/IpgC Proteins Following Purification

Proteins were placed in dialysis tubing. All dialysis steps conducted at 4°C. IpaB/IpgC dialyzed in five steps.

1. Against 1X wash buffer for 1 hour.
2. Against 1X binding buffer for 2 hours.
3. Against 500mM NaCl PBS overnight.
4. Against 300mM NaCl PBS for 1 hour.
5. Against 1X (200mM NaCl) PBS for 1 hour.

Purified protein was then removed from dialysis tubing, placed into a 1.5 ml eppendorf tube and stored at 4°C for up to two weeks.

Dialysis of IpaB Following Purification

Proteins were placed in a Thermo Scientific Slide-A-Lyzer dialysis cassette, 3 ml to 12ml volume, with a syringe and 21 gauge needle. All dialysis steps were done at 4°C. Cassettes were dialyzed against 500 ml of NaP dialysis buffer for 30 minutes, then 500 ml of fresh NaP dialysis buffer overnight. The protein was then removed from the cassette and the concentration was determined by A_{280} UV absorbance using the equation

C (concentration) = (absorbance) / (extinction coefficient)

with an extinction coefficient=11,460 for IpaB.

Determining the Tryptophan Fluorescence Emission Maximium

Fluorescence data were collected using a Fluoromax-4 Spectrofluorometer scanning fluorescence spectrophotometer. The machine was adjusted with a blank that consisted of 0.6 ml PBS. Tryptophan (Trp) fluorescence emission was scanned at wavelengths from 305 nm to 400 nm using an excitation wavelength of 295 nm, which allowed for monitoring of changes in tryptophan emission between IpaB/IpgC and IpaB alone, as well as allowing the comparison of the environments surrounding each Trp for all the mutants and the wildtype. Other settings included a tolerance of 1°C, an equilibration time of three minutes, and a temperature of 20°C. Three scans

were taken for each sample with the resulting graph representing an average of the three scans.

Tryptophan Thermal Unfolding Curves

Thermal unfolding data were collected using a Fluoromax-4 Spectrofluorometer scanning fluorescence spectrophotometer. The machine was adjusted with a blank that consisted of 0.6 ml PBS. For all the proteins, fluorescence emission was scanned at wavelengths from 305 nm to 400 nm using an excitation wavelength of 295 nm, which allowed for monitoring changes in tryptophan emission between IpaB/IpgC and IpaB alone, as well as allowing the comparison of the environments surrounding each Trp for all the mutants and the wildtype. Other settings included an equilibration time of three minutes and a temperature range from 10°C to 90°C increasing at increments of 2.5°C, with a tolerance of 1°C from 10°C to 57.5°C and 1.5°C from 60°C to 90°C.

IAEDANS Labeling of IpaB

Protein concentrations were determined by A_{280} UV absorbance using the equation C (concentration) = (absorbance)/(extinction coefficient), with an extinction coefficient=11,460 and MW of 62,000 Da for IpaB. β-mercaptoethonal (BME) was added to the purified protein to a concentration of 25 μM and the sample was allowed to sit on ice for one hour. To remove the BME, the proteins were placed in Slide-A-Lyzer cassettes, 3 ml to 12 ml volume, and dialyzed against four rounds of 500 ml of NaP buffer for 30 minutes each at 4°C. The sample was removed from dialysis and labeled with 5-[2-[(2-Iodo-1-

oxoethyl)amino] ethylamino]-1-naphthalenesulfonic acid (IAEDANS). Approximately 1 mg of IAEDANS was mixed with 125 µl of dimethyl sulfoxide (DMSO) and this was added to the protein, which was allowed to sit for one hour on ice. Protein samples were again purified using the Ni+ affinity chromatography with OPOE as previously described. Fractions were collected and SDS-PAGE was used to determine the fractions that contained protein. These fractions were pooled and dialyzed against the NaP buffer using four rounds of 500ml for 30 minutes each at 4°C in Slide-A-Lyzer cassettes. Samples were then removed form the cassettes and used for scanning in Förster resonance energy transfer studies.

Förster Resonance Energy Transfer (FRET) with AEDANS-Labeled IpaB

FRET data were collected using the Fluoromax-4 Spectrofluorometer scanning fluorescence spectrophotometer. The machine baseline was set with 0.6 ml of PBS. Samples were excited at a wavelength of 290 nm and scanning emission wavelengths were collected from 300 nm to 500 nm, with 1°C tolerance, three minute equilibration times and a starting temperature of 20°C. Samples were scanned separately using the same concentration of unlabeled (donor only) and labeled (donor/acceptor) protein. Graphs shown here are average of each after three scans. The emission maximum intensity of the unlabeled protein relative to the intensity of the labeled protein at the same wavelength was compared. The difference between the emission maximum of the donor (Trp) only sample and the emission maximum of the donor/acceptor

(Cys309+AEDANS) sample at the donor max wavelength allows the amount of energy transfer to be calculated.

For each mutant and the native strain, the energy transfer efficiency was calculated according to the equation:

$$E = (1-(Fda/Fd))$$

where Fda = donor/acceptor intensity and Fd = donor intensity. After determining the amount of energy transferred, the distance between the tryptophan and the molecule of AEDANS on Cys309 was calculated using the formula:

$$E = (R_o^6)/(R_o^6+R^6)$$

where R is the calculated distance separating the donor and acceptor fluorophores. The published R_o value for this donor-acceptor fluorophore pair is 22Å, which is the theoretical distance that would give 50% energy transfer efficiency (R_o) for this specific FRET pair (Lakowicz, 2006). When determining the R_o value, it was assumed the orientation of donor and acceptor dipoles are random ($\kappa^2=2/3$). This is a standard assumption.

CHAPTER III

TRYPTOPHAN SCANNING MUTAGENESIS OF IpaB

Introduction

Shigella flexneri uses its type III secretion system (TTSS) to facilitate its own uptake in the colonic epithelial cells of the large intestine (Sansonetti *et al.*, 1982b). Once the *S. flexneri* TTSS is activated by contact with a host cell (or conditions mimicking host cell contact) it begins to transport effector proteins through its extracellular needle apparatus into the host cell's membrane and cytoplasm (or into the extracellular environment). After secretion activation, IpaB is secreted into a position within the host cell membrane followed by IpaC. These proteins act as early effectors of *Shigella* invasion. These two proteins associate within the host cell membrane where they form a translocon pore that allows other (later) effector proteins to pass directly into the host cell's cytoplasm where they can contribute to bacterial invasion (Davis *et al.*, 1998) (Blocker *et al.*, 1999). Without the translocon pore inserted on the basolateral face, *S. flexneri* cannot enter the host cell (Menard *et al.*, 1993). To prevent premature secretion of its translocators, *Shigella* stores IpaB and IpaC in the bacterial cytoplasm

where they are bound to the chaperone IpgC. As part of this complex, they are stored until the specific signals to be secreted by the TTSS are received by the bacterium (Menard *et al.*, 1993) (Menard *et al.*, 1994) (Page *et al.*, 1999).

IpaB

IpaB is a large translocator/effector molecule that possesses multiple functions and is secreted by the TTSS of *Shigella flexneri*. Its functions include directing apoptosis (pyroptosis) in macrophages as a secreted effector and as a translocon structural protein through its interaction with IpaC. The translocon pore is inserted into the host cell's membrane to allow additional effector proteins to be directly secreted into the host cell's cytoplasm (Menard *et al.*, 1994) (Zychlinsky *et al.*, 1994) (Blocker *et al.*, 1999). There is currently no structural information available for IpaB and this is mostly due to its large molecular size (62 kDa) and hydrophobic nature (Birket *et al.*, 2007). The entire amino acid sequence of IpaB, 580 residues, has been divided into predicted regions based on protein structure algorithms, some functional data, and the known structure of IpaD to which it has been compared (W.L. Picking unpublished observations)(Guichon *et al.*, 2001). Based on experimental data and predicted protein properties, IpaB can be divided into six regions. These regions include a N-terminal helix-turn-helix, two regions that form a dimeric coiled-coil, two transmembrane helices and a region predicted to lie on the inner face of the host cell membrane (Figure 3.1). Guichon *et al.* performed structure function analyses of IpaB and determined that protein expression was

stopped with the introduction of large deletions within the N-terminus (Guichon *et al.*, 2001). Guichen *et al.* also determined that expression of IpaB was not impaired when large deletions were introduced within the C-terminus, however, a significant decrease in (or total loss of) invasiveness, cell cytotoxicity and phagosomal escape was seen (Guichon *et al.*, 2001). They also introduced small deletions within the putative transmembrane region, many of which had little effect on protein function or expression when compared to the wildtype (Guichon *et al.*, 2001). They did find one deletion that had a significant effect on protein function and expression which consisted of amino acids 307-316, and are the seven amino acids immediately preceding the transmembrane/hydrophobic region and the first three amino acids of the region (Guichon *et al.*, 2001). When expressed in *S. flexneri,* the mutant 307-316, had significantly less expression of IpaB, it was unable to lyse the phagosome or induce macrophage cell death (Guichon *et al.*, 2001). Their results indicated that the binding site for caspase 1 is contained in the hydrophobic region, as a mutant lacking amino acids 311-580 was unable to bind caspase 1, however, a mutant with amino acids 307-316 deleted was able to bind caspase 1 but could not induce macrophage apoptosis (Guichon *et al.*, 2001). The worked performed by Guichon *et al.* demonstrates that IpaB's N-terminal is necessary for stable expression and function of the protein, the hydrophobic region is needed to maintain function of IpaB or to keep other domains in a proper confirmation for expression, and that IpaB binding of caspase 1 alone is not sufficient to induce macrophage apoptosis but is only the first step (Guichon *et al.,* 2001).

	N-Terminal Helix-turn-helix
	Dimeric Coiled Coil
	Transmembrane Helices
	Region predicted to lie on the inner face of the host cell membrane

Figure 3.1 Predicted IpaB Organizational Map
This organizational map is based on the known structure of IpaD (Wendy Picking, unpublished).

IpaB's Interaction with IpgC

Before IpaB is secreted by the Shigella TTSS, it waits in the bacterial cytoplasm bound to its molecular chaperone IpgC (Birket *et al.*, 2007). IpgC is a class two molecular chaperone specific for binding both IpaB and IpaC (Birket *et al.*, 2007). By binding to IpaB and IpaC, IpgC prevents the degradation of the two translocator proteins that would result if these two pore components became associated while still in the bacterial cytoplasm (prior to secretion). It is also thought that IpgC is responsible for maintaining IpaB in a state of readiness for secretion through the TTSS needle apparatus (Page *et al.*, 1999). After release from IpaB and IpaC, IpgC then binds to the transcription activator *mxiE* to allow the expression of later effector proteins that are injected into the host cytoplasm following bacterial invasion (Mavris *et al.*, 2002).

Circular Dichrosim Spectroscopic Analysis of IpB/IpgC and IpaB

Circular dichrosim (CD) spectroscopy can be used to determine the overall secondary structure of a protein. It uses circularly polarized light and measures the differences in the absorption of left and right handed polarized light (Whitmore and Wallace, 2004). CD spectroscopy utilizes the "far-UV" spectral region (190-250 nm) to determine information about the global secondary structure (Whitmore and Wallace, 2004) (Espina *et al.*, 2007). Using this wavelength region, the peptide bond serves as the chromophore exhibiting specific positive and negative signals when its environment is regular and folded

(Whitmore and Wallace, 2004). This method allows the type and amount of secondary structure a protein contains to be determined because these different secondary structures (including alpha-helix, beta-sheet, and random coil) have a characteristic CD spectrum. This method cannot, however, be used to determine the specific residues involved in any of the three aforementioned types of secondary structure within a protein. CD analysis of IpaB/IpgC and IpaB alone (performed by N. Darboe) reveals that IpgC has a significant effect on the secondary structure of IpaB (Figure 3.2). Both IpaB/IpgC and IpaB alone have significant alpha-helical structure supported by the characteristic minima at 208 and 223 nm. While the IpaB/IpgC complex is slightly more structured (more α-helical) when compared to IpaB alone, IpgC is not necessary for IpaB to matain its structure.

Fourier Transform Infrared Spectroscopy

Fourier transform infrared spectroscopy (FTIR) can be used to determine the types of chemical bonds a sample contains by creating an infrared absorption spectrum (Espina *et al.*, 2007). It does this by measuring the specific wavelengths absorbed when a sample is exposed to infrared radiation (Gallagher, 2005). FTIR analysis of IpaB (performed by C. Olsen) displayed a characteristic pattern consistent with a protein having a dimeric coiled-coil (Figure 3.3). These data, along with the CD analysis, support the hypothesis that IpaB is a highly structured protein.

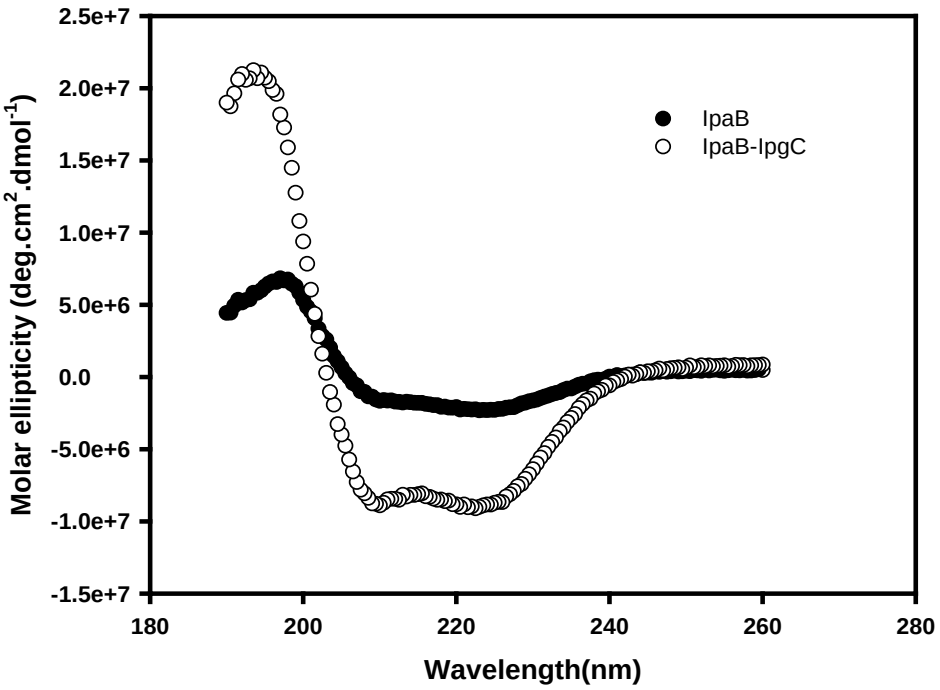

Figure 3.2 CD Spectra of IpaB/IpgC and IpaB
This CD spectrum shows both IpaB (filled circles) and IpaB/IpgC complex (unfilled circles) have significant alpha helical components with characteristic minima at 208 nm and 223 nm (performed by N. Darboe).

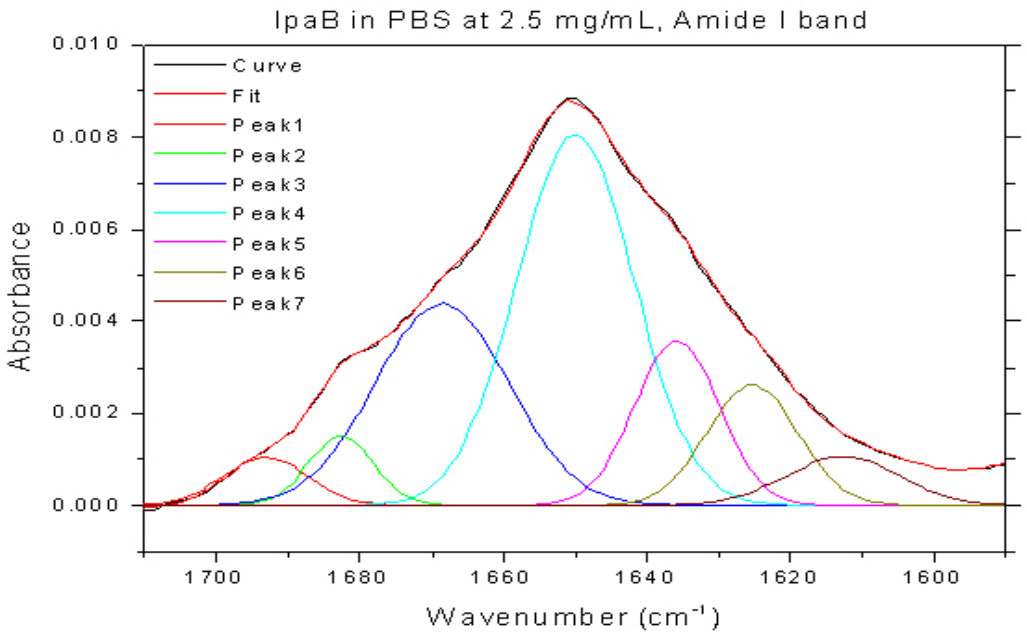

Figure 3.3 Fourier Transform Infrared (FTIR) Spectrum of IpaB
The IpaB FTIR spectrum has the characteristics of a protein with a dimeric coiled-coil (performed by C. Olsen).

In this study, fluorescence spectroscopy was utilized to ascertain the effects of IpgC binding on IpaB and to make a first ever attempt at determining a topological map for Trp residues within the protein. Tryptophan scanning mutagenesis has been utilized previously to efficiently determine the effect of IpgC binding on IpaC. We have utilized these same techniques to better define regions of IpaB that are affected by the binding of IpgC along with its secondary structure and topology. Because so little structural information is available for IpaB, this will provide new details on its structure so that can be used for future mutagenesis studies.

Results

Construction of Insertion Mutants

Previously, members of the lab have used tryptophan scanning mutagenesis to characterize the effects on the structure and the microenvironments of regions of IpaC following protien binding to liposomes and to the IpgC chaperone (Harrington *et al.*, 2006) (Birket *et al.*, 2007). For proteins containing only a single Trp residue, Trp scanning mutagenesis exploits the natural environmental sensitivity of the single indole group of the Trp to gain information on its local surroundings. Trp fluorescence is highly sensitive to the polarity of the environment immediately around it. This method allows fluorescence differences for a protein in two different states to be analyzed for the influence these states have on a single residue within the protein. In this

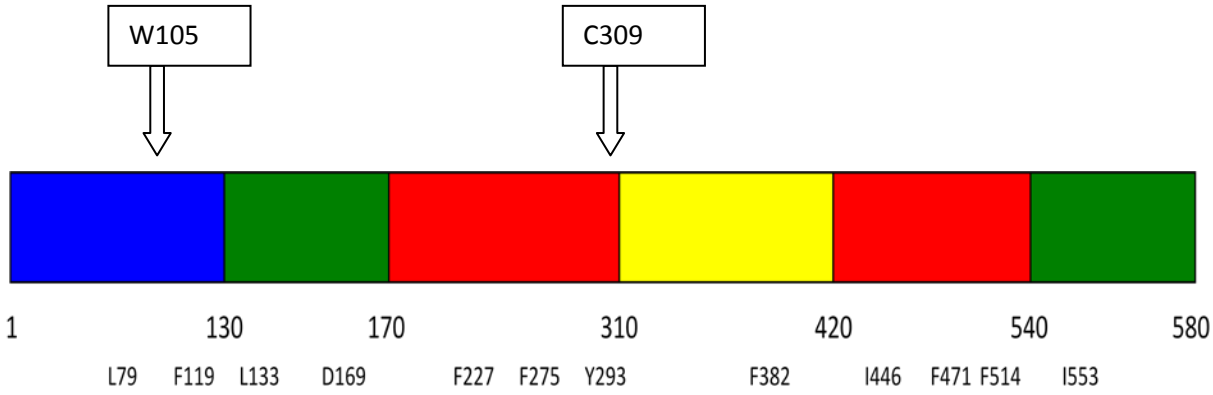

	N-Terminal Helix-turn-helix
	Dimeric Coiled Coil
	Transmembrane Helices
	Region predicted to lie on the inner face of the host cell membrane

Figure 3.4 Predicted IpaB Organizational Map
This organizational map based on the known structure of IpaD shows the predicted regions of IpaB and the placement of the single Trp insertion mutants with the native Trp at residue 105 and the single Cys at residue 309 labeled (Wendy Picking, unpublished observations).

case, the influence of IpgC binding to IpaB can be used to determine how complex formation affects specific regions within IpaB (whereever a Trp residue has been inserted).

Trp scanning mutagenesis with fluorescence characterization of the resulting mutant requires that the protein possess only a single tryptophan. Wildtype *ipaB* contains a single Trp residue residing at position 105 (Figure 3.4). In previous studies with IpaC it was convenient that the protein does not have a natural Trp so one could simple be inserted any where (Birket *et al.*, 2007). A library of IpaC mutants having only a single Trp were thus made by inserting a Trp at perceived key positions (Birket *et al.*, 2007). The lack of a natural Trp made the creation of point mutations in IpaC easy (Birket *et al.*, 2007).

The natural Trp of IpaB at residue 105 allowed for the N-terminal region to be characterized. Before other regions could be studied, however, this natural Trp needed to be removed. A knockout mutant was thus created with the natural Trp at residue 105 replaced with a phenylalanine (Phe). The remaining point mutations were based on this W105F IpaB mutant template (IpaB ΔW).

Site-directed mutagenesis was used to generate 12 mutants that contained single Trp residues spanning the length of IpaB. This allowed the use of fluorescence spectroscopy to characterize the entire length of the protein (Picking *et al.*, 1996). In addition to the natural Trp at residue 105, mutants were generated that had individual Trp residues introduced at positions 81, 119, 133, 169, 227, 275, 293, 382, 446, 514, and 553. Positions 81, 105 and 119 are in the predicted N-terminal helix-turn-helix (Fig. 3.1). Positions 133, 169 and 553

Mutant	Primer Name and Sequence
L79W	B88f-GAGAGAGAGGCTAGCTCCCAATGGACGCTTTTAATTGGAAACC
	B89r-GAGAGAGAGGCTAGCATTTAATGACTTTGGTGCTTT
F119W	B90f-GAGAGAGAGCTCGAGTGGTCCGATAAAATTAACAC
	B91r-GAGAGAGAGCTCGAGGTTTTTTTGCTGTCTTG
L133W	B53f-GAGAGAGAGACGCGTGACTATGAAAAACAAATTAATAA
	B54r-GAGAGAGAGACGCGTCCATCCTTCAGTTTCAGATAGAA
D169W	B92f-GAGAGAGAGTGGCCAGAGTCACCAGAAAAG
	B93r-GAGAGAGAGTGGCCAGAGGTTCGATAATCTTGTTTG
F227W	B94f-GAGAGAGAGGCTAGCGCTGAACAGCTATCAAC
	B95r-GAGAGAGAGGCTAGCTGTGTTTGACCATGCAGAAAAAGAGTC TATTT
F275W	B96f-GAGAGAGAGCTTAAGAATGATCTGGCTCTATGGCAGTCTCTC CAAGAATCAA
	B97r-GAGAGAGAGCTTAAGAGATTCTTCATTATTTTTTCCA
Y293W	B110f-GAGAGAGAGTACGTAAAGCAGAAGAACTC
	B99r-GAGAGAGAGTACGTACTTCAGCAGCCCACTCATCAGATTTTC TCTC
F382W	B100f-GAGAGAGAGCTCGAGGGCTTGGGCGTCGATC
	B101r-GAGAGAGAGCTCGAGCATTTTTGTCCATGCATCTGAAAGG AGTTT
I446W	B102f-GAGAGAGAGTGGCCAAAGTTTCTCAAGAATTTT
	B103r-GAGAGAGAGTGGCCAAAGGTCTGTGAGGGTTTTA
F471W	B104f-GAGAGAGAGGCCGGCGATGAAGTAATATCCAAACA
	B105r-GAGAGAGAGGCCGGCTGCACCAAGCCATTTATTTAATCTGGC AACAC
F514W	B106f-GAGAGAGAGGCTAGCGACAAATCTAGCAGACCT
	B107r-GAGAGAGAGGCTAGCGCTGTTCTGCCAAACAGCAGAAGCGA CACT
I553W	B108f-GAGAGAGAGAGATCTATTAGCCTCAATGT
	B109r-GAGAGAGAGAGATCTGCCCATACTTCCTGCAATTGGC

Table 3.1 Table of Primers
This table list the primers used with the ΔW template to create the single Trp insertion mutants.

are located in the predicted dimeric coiled-coil. Positions 227, 275, 293, 446, 471, and 514 are contained in the predicted transmembrane helices. The final mutant contained a Trp at position 382 which is within the region predicted to lie on the inner face of the host cell membrane following insertion of the pore by the bacterium. The specific primers used to generate these mutants are listed in Table 3.1. These were double mutants made using the point mutation W105F as a template to ensure each mutant had a lone Trp residue. In order to minimize changes in IpaB's structure and function, the amino acids most often targeted for mutagenesis contained bulky side chains and were non-polar (hydrophobic), including leucine, isoleucine, tyrosine and phenylalanine.

Analysis of Trp Replacement Using Invasion and Hemolysis Assays

Invasion and contact-mediated hemolysis assays were performed to determine the effects of replacing the native Trp and introducing Trp residues into other regions within IpaB. Invasion is a measure of the bacteria's ability to invade a host cell while contact-mediated hemolysis is a measure of the bacterium's ability to form a translocon pore and insert it into the host cell membrane.

The results for invasion and hemolysis for the *S. flexneri* strain SF620 expressing wildtype IpaB were used to provide a baseline of activity for comparison with all the mutants created to determine if the specific mutation had an effect of the function of IpaB. As is reported in Table 3.2, the wildtype IpaB had a relative invasiveness of 100% and hemolysis of 100%. Results below 50%

Trp Mutant	Relative Invasion, %	Contact Hemolysis, %
IpaB/IpgC	100	100
IpaB ΔW/IpgC	89	95
IpaB L79W/IpgC	280	82.20
IpaB F119W/IpgC	106	89.70
IpaB L133W/IpgC	0	83.50
IpaB D169W/IpgC	98	78.90
IpaB F227W/IpgC	0	65.50
IpaB F275W/IpgC	0	0
IpaB Y293W/IpgC	0	0
IpaB F382W/IpgC	0	1.40
IpaB I446W/IpgC	17	13.
IpaB F471W/IpgC	0	37.40
IpaB F514W/IpgC	ND	ND
IpaB I553W/IpgC	0	0

Table 3.2 Functional Analysis of the IpaB Single Trp Mutants Produced in *S. flexneri*

A significant change was determined to be less than 50% of the wildtype IpaB/IpgC invasiveness and hemolysis results. All results were within 10-15% of the results given in the table. ND-No data available due to the construct not producing the proper size protein

of the wildtype IpaB value were determined to be a significant decrease. IpaB ΔW with the native Trp removed, did not show a significant decrease in invasiveness or hemolysis, 89% and 95%, respectively. This shows that the removal of the native Trp at residue 105 and its replacement with Phe had little negative effect on the function of IpaB. These results demonstrated that the IpaB ΔW mutant could then be used as a template to make other mutants by inserting a Trp at different locations.

The invasion and hemolysis assays were performed on the twelve mutants created (Table 3.2). Three of the mutants, L79W, F119W and D169W, showed no significant decrease in invasiveness, while L79W and F119W showed an increase in invasiveness. Most of the mutants, F227W, F275W, Y293W, F382W, I446W, F471W and I553W, showed zero invasiveness with I446W having only 17% invasiveness. The mutants L79W, F119W, L133W, D169W and F22W did not have a significant decrease in hemolysis. The remaining mutants, F275W, Y293W, F382W, I446W, F471W and I553 all had significant decreases in hemolysis with three mutants, F275W, Y293W and I553W having zero hemolysis activity. These results suggest that some of the mutations in IpaB have little to no impact on its function but some of the insertions do have a significant impact of the invasiveness and hemolysis of IpaB, however they have not significantly changed the overall structure of the protein. Invasion and hemolysis data are not available for F514W due to a problem with the construct not producing the proper size protein.

Three of the mutants, F227W, I446W and F514W, had problems with transformation and expression based on western blot analysis (data not shown). It was determined that there had been a problem in the original transformation as the three mutants were not producing protein when the cultures were grown. These three mutants were retransformed and thought to produce protein, however, after analysis of the sodium dodecyl sulfate-polyacrylamide gel electrophoresis (SDS-PAGE) gels, it was determined that the bands on these three gels were not the right size to be IpaB (62 kDa). Thus, it was determined that there was again a problem with the expression of these three mutants and that any data collected before this problem was identified should be discarded. It was also decided these three mutants would not be used in the fluorescence experiments that follow.

Tryptophan Emission Maxima Fluorescence

Recombinant IpaB was purified with IpgC as a soluble complex in *E. coli* as was previously done with IpaC/IpgC (Birket *et al.*, 2007). To better characterize key regions within IpaB and determine regions that might undergo a significant conformational change upon release from IpgC or which might physically interact with IpgC, Trp scanning mutagenesis was performed to allow comparison of the emission properties of the IpaB/IpgC complex with IpaB alone for the wildtype protein and nine mutants. For this experiment, the wildtype IpaB as well as the nine mutants with His-tag labeled IpaB were grown in 1L cultures of *E.coli* Tuner (DE3) cells to an OD=0.6 at 600 nm. At this time the cells were

inoculated with isopropyl-thio-2-D-galactopyranoside (IPTG) to induce protein production (Page *et al*, 1999). IPTG is a non-metabolized *lac*-inducer added to cultures to induce recombinant protein expression when the gene is under the control of a *lac* promoter (Page *et al.*, 1999). This method allows for the production of large amounts of protein that can be subsequently harvested and purified (Page *et al.*, 1999). This method utilized the Tuner cells to produce the recombinant IpaB protein by inducing co-expression of the IpaB/IpgC complex. After induction with IPTG, the cells continued to shake at 37°C for three hours, at which time they are removed and collected by centrifugation at 4000 rpm for 15 minutes. The supernatant fraction was discarded and the pellet containing the bacteria was resuspended in 40 ml of 1X binding buffer. The suspension was placed in a freezer bottle and stored in a -20°C freezer for later use. After freezing overnight, the suspension was removed and placed in a 37°C water bath until completely thawed. The liquid was then transferred to a beaker on ice to prevent the protein from overheating during sonication. The liquid containing the bacteria was sonicated for approximately one minute and thirty seconds per liter of original culture grown. After sonication Ni+ affinity column chromatography was used to purify the protein. The IpaB/IpgC complex bound to the column via the His-tag on IpaB while everything else passed through. The IpaB/IpgC complex was then eluted from the column and collected in 1.5 ml fractions. The fractions were then run on a SDS-PAGE gel to determine which fractions contained the IpaB/IpgC complex (Figure 3.5). IpgC's band is much lower on the gel than IpaB due to its small size (20 kDa). The fractions that contained the

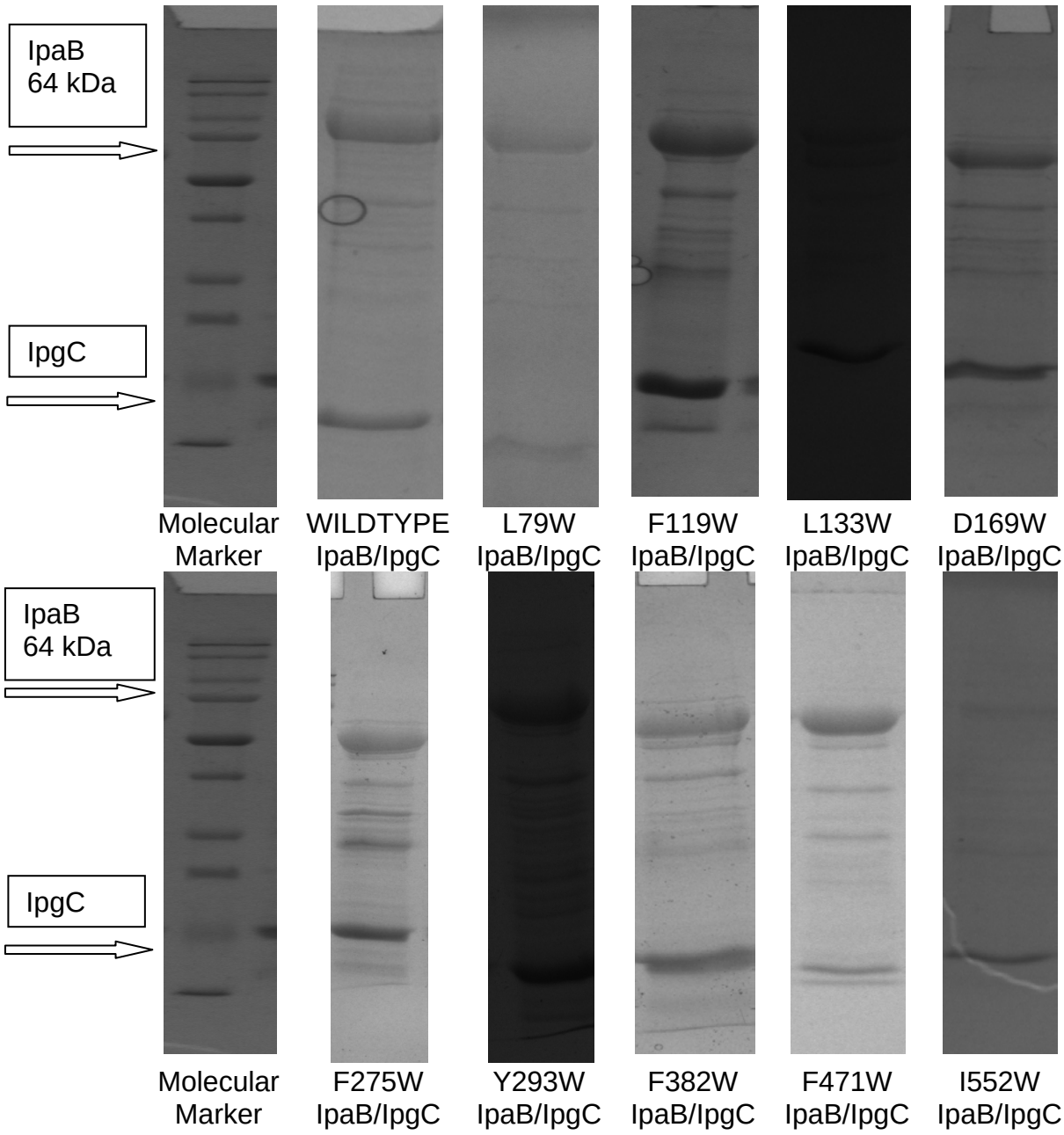

Figure 3.5 Purified IpaB/IpgC
Gels of IpaB/IpgC samples display the IpaB band at approximately 64 kDa and the IpgC at approximately 20 kDa. The SDS-PAGE gel (12%) was stained with Coomassie blue dye.

most IpaB/IpgC complex were pooled to be used for future fluorescence analysis. In order to leave as much protein as possible for studying IpaB alone and for labeling the Cysteine (Cys) residue in later experiments, only one-fourth of the total amount of original culture grown was used for analysis of the IpaB/IpgC complex.

The remaining three-fourths of the protein preparation was poured over the column with the IpaB/IpgC again bound to the Ni+ affinity chromatography column. Before eluting the column, however, binding buffer with 1% OPOE, a mild detergent, was added and the column was allowed to sit in a cold room at 4°C overnight on a rocker plate at half speed. This was done because the IpaB/IpgC complex can be separated in the presence of this detergent (Birket *et al.*, 2007). Hume *et al.* have shown that IpaB can be purified from IpgC in *E. coli* using a mild detergent (Hume *et al.*, 2003). After allowing the column to sit overnight, it was washed to remove the IpgC that had become separated from IpaB. The column was eluted as before (with imidazole) to collect IpaB fractions. This method allowed the collection of IpaB alone due to the His-tag it contains, while the free IpgC should pass through the column. These fractions were also run on a SDS-PAGE (12%) gel to determine if the IpgC had been released (Fig. 3.6). Theoretically, all the IpgC should be released from the complex and contained in the flow through prior to imidazole elution. A sample of the flow through was also run to determine that IpgC had indeed released and was no longer complexed with IpaB (data not shown). After pooling the IpaB only fractions, some of it was frozen in a -80°C freezer to be used for later

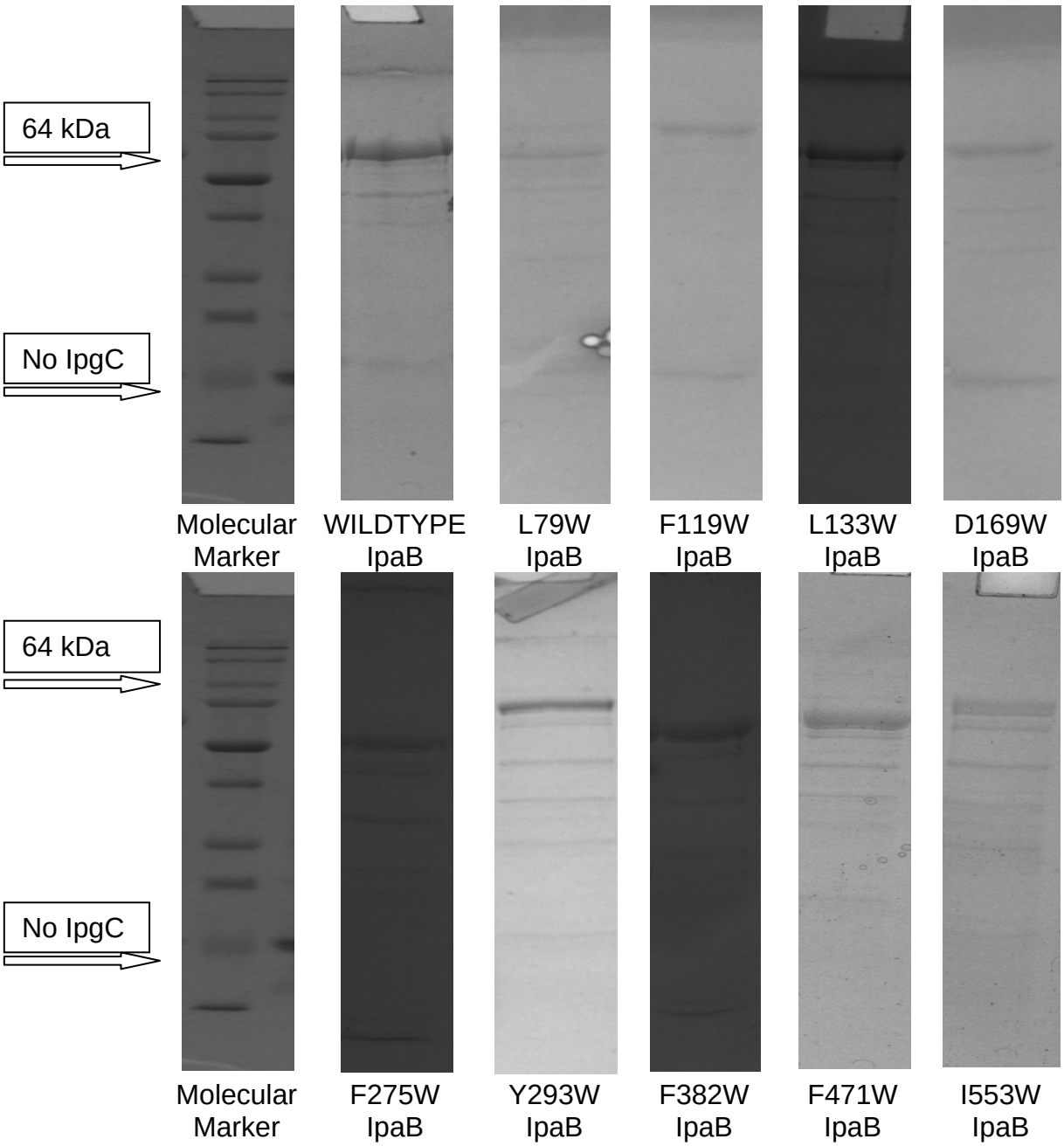

Figure 3.6 Gels of Purified IpaB After Removal of IpgC
This Commassie-blue stained SDS-PAGE gel shows that the samples contains the IpaB (64 kDa) purified away from IpgC following inoculation with OPOE.

fluorescence labeling and energy transfer studies.

Emission maxima values for all of the recombinant IpaB proteins (with and without IpgC) are shown in Table 3.3. For these experiments it was determined that a significant change was any wavelength shift equal to or greater than 5 nm in either direction, red or blue. A red shift is a shift to a longer wavelength indicating the environment around a specific Trp has become hydrophilic and more polar (Sams *et al.*, 1977). A blue shift is a shift to a shorter wavelength indicating the environment around a specific Trp has become more hydrophobic and less polar (Sams *et al.*, 1977). A red shift would indicate movement of the residue into a less buried or more exposed state while a blue shift would be due to a residue becoming more buried within the structure of the protein. Both shifts could be due to a conformational change of the entire protein or within a specific region or microenvironment induced by the binding of IpgC. If comparing the IpaB/IpgC wild type to the IpaB/IpgC mutants or the IpaB only wildtype to the IpaB only mutants the shifts are likely due to the environment around the specific Trp being different than the native Trp105

The purified IpaB/IpgC complex and IpaB alone were both scanned on a spectrofluorometer. Sample graphs displaying emission maximum scans of wildtype IpaB complexed with IpgC and wildtype IpaB alone are shown in Figures 3.7 and 3.8, respectively. The IpaB/IpgC complex displayed an emission maximum of 332 nm while IpaB not bound to IpgC displayed an emission maximum of 337 nm. This shift (of 5 nm) is a significant shift, as previously defined, indicating that the environment around the Trp at residue 105 becomes

more hydrophilic and more polar in the absence of IpgC. This could be due to IpgC contacting this Trp or the binding of IpgC may induce a conformational change in the region that buries the Trp within the protein.

The results of all emission maxima scans are shown in Table 3.3. First, the emission maximum of the IpaB only mutants will be compared to the wildtype IpaB only emission maximum to determine differences in the environments around the inserted Trps. Of the nine IpaB mutants, eight displayed a spectral shift compared to IpaB 105W. Mutants L79, F275, F382, and I553 all displayed a blue shift or a shift to a shorter wavelength compared to the wildtype IpaB only. This indicates that the environments around these Trp residues became more hydrophobic and less polar compared to the wiltype IpaB only. Mutants L79, F275 and F382 displayed significant shifts of 8 nm, 10 nm, and 15 nm, respectively. This indicates that the microenvironments around these Trp residues are more buried within the protein than the native Trp. The mutants F119, D169, Y293, and F471 all displayed a red shift or a shift to a longer wavelength, indicating that these Trp residues are in a hydrophilic and more polar environment than the native Trp of IpaB only. Only one, D169, displayed a significant red shift of 9 nm. The region containing this residue is significantly less buried than the native Trp. The mutant L133 did not display a spectral shift in either direction, meaning its microenvironment is similar too or the same as the microenvironment of the native Trp.

Second, the emission maximum of the mutants IpaB/IpgC complexes ill be compared to the wildtype IpaB/IpgC emissions maximum to again determine

differences in the regions surrounding the inserted Trps. Four of the IpaB only Trp mutants, L79, F275, F382, and I553, displayed a blue shift compared to the wildtype IpaB/IpgC complex. This indicates that the area around these Trp residues is more hydrophobic and less polar than the native Trp. Three of the mutants, F275, F322 and I553, displayed a significant shift to a shorter wavelength, 5 nm, 10 nm and 8 nm, respectively. This is likely due to these regions being more buried within the structure of the folded protein compared tot eh wildtype IpaB/IpgC Trp. The remaining five mutants, F119, L133, D169, Y293, and F471, all displayed a red shift or a shift to a longer wavelength, indicating these microenvironments are hydrophilic and less buried relative to the native Trp of the IpaB/IpgC complex. Two of the mutants, F119 and D169 displayed significant red shifts, 11 nm and 13 nm, respectively. These shifts are likely due to these two regions being significantly more exposed or less buried with the structure of the protein relative to the wildtype IpaB/IpgC complex.

Third, the emission maximum of the IpaB/IpgC complex will be compared to IpaB alone, for each mutant. Of the nine mutants, only two displayed a significant spectral shift. The remaining seven mutants, L81, F119, L133, D169, F275, Y293 and F382, did not display a significant spectral shift when not bound to IpgC (Table 3.3). This indicates that the environments around these Trp residues are not significantly altered during IpaB binding with IpgC or they do not undergo a conformational change that transforms the environment around these particular Trp residues which can be detected by this method. Both, F471 (7 nm) and I553 (9 nm) displayed a significant red shift when not bound to IpgC. As

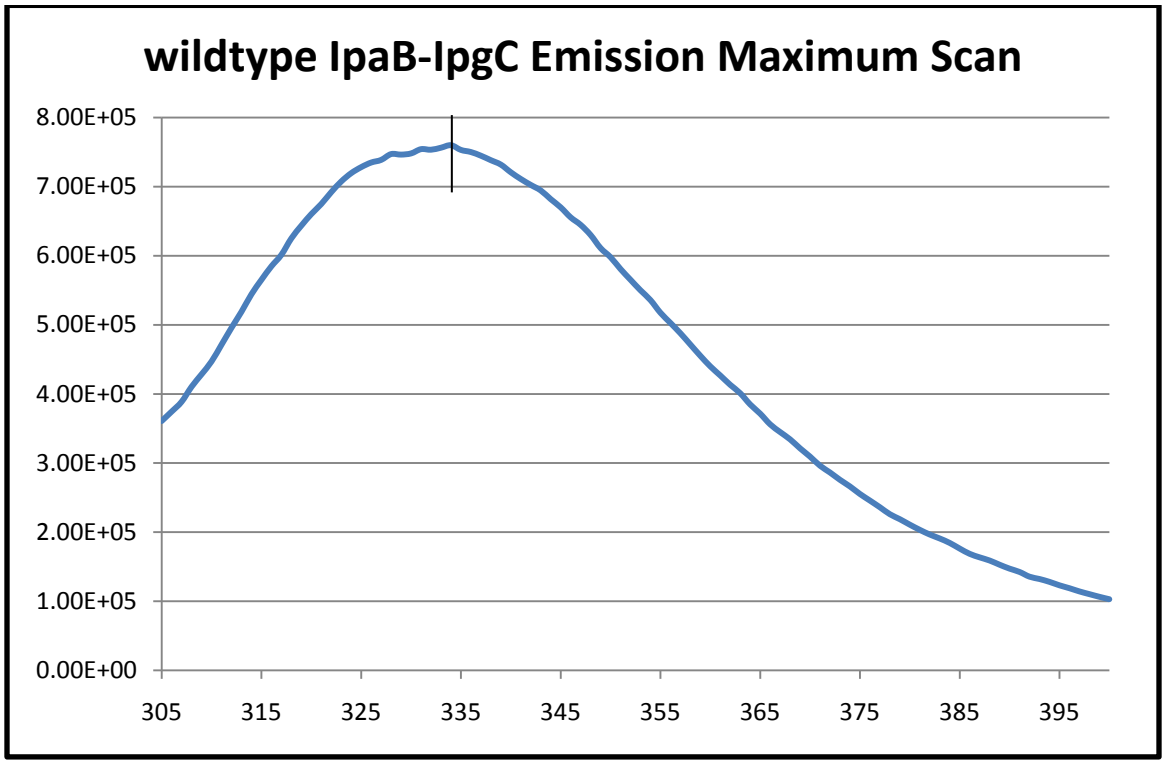

Figure 3.7 Emission Maximum Scan of wildtype IpaB/IpgC Complex
The wildtype sample was excited at 295 nm and the spectrum collected at a scanning range of 305 nm to 400 nm at a rate of 0.1 sec per increment of 1 nm.

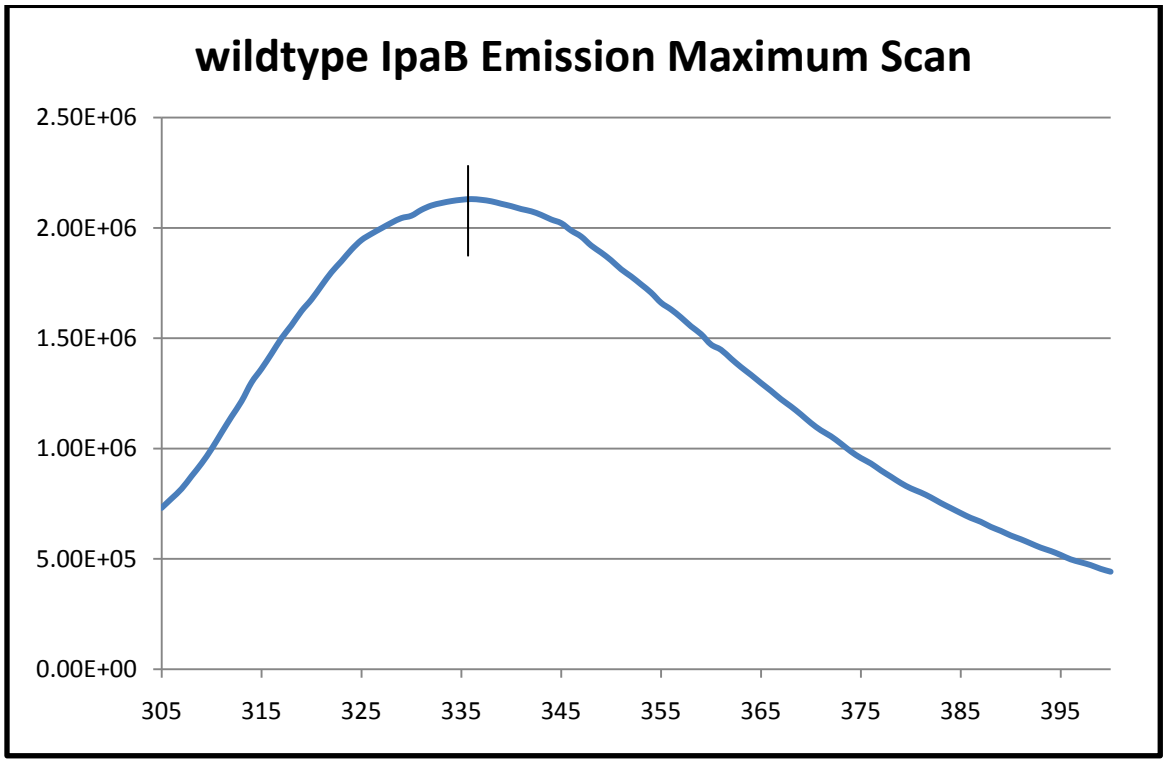

Figure 3.8 Emission Maximum Scan of wildtype IpaB without IpgC
The wildtype sample was excited at 295 nm and the spectrum collected at a scanning range of 305 nm to 400 nm at a rate of 0.1 sec per increment of 1 nm.

Trp Mutant	Emission Maximum, nm
IpaB/IpgC	332
IpaB	337
IpaB L79W/IpgC	328
IpaB L79W	329
IpaB F119W/IpgC	343
IpaB F119W	341
IpaB L133W/IpgC	336
IpaB L133W	337
IpaB D169W/IpgC	345
IpaB D169W	346
IpaB F275W/IpgC	327
IpaB F275W	327
IpaB Y293W/IpgC	335
IpaB Y293W	339
IpaB F382W/IpgC	322
IpaB F382W	322
IpaB F471W/IpgC	334
IpaB F471W	341
IpaB I553W/IpgC	324
IpaB I553W	333

Table 3.3 Mutational Characteristics of Single Trp Mutants
This table lists the emission maximum for each individual sample. A significant shift was considered to be any shift of 5 nm or more in either the red or the blue.

previously stated the wildtype IpaB (W105) also displayed a significant shift upon IpaB binding (5 nm, as shown in Table 3.3). It is interesting to note that all three displayed a red shift upon removal of IpgC, indicating the environment around these Trp residues became more polar and hydrophilic. These data suggest that these three residues, or the specific regions containing them, may be either directly involved in binding IpgC or the region undergoes a significant and detectable conformational change exposing the environments making them hydrophilic which results in the observed change in Trp fluorescence. The wildtype IpaB has a Trp at residue 105 and lies in the predicted N-terminal helix-turn-helix region. F471 resides in the predicted transmembrane helix nearest the C-terminal. I553 is contained in the second or C-terminal coil of the predicted dimeric coiled-coil. We speculate that IpgC may interact with IpaB at these areas to maintain it in a secretion ready state, however, we cannot rule out that these regions undergo a conformational change after dissociation from IpgC either to pass through the narrow inner channel of the TTSA needle, to prepare for binding/interaction with IpaC, or to assume an active effector state. The fluorescence method used here is well suited for determining information about the environments immediately surrounding Trp residues, but it does not provide a global picture of the effects of the binding of a chaperone to its cognate protein.

Thermal Unfolding Analysis of IpaB/IpgC and IpaB

To determine the effect of IpgC binding on the thermal stability of the various environments surrounding each specific Trp insertion, thermal unfolding

analyses were performed. As with the emission maxima determinations, this method does not provide a global picture of the protein's stability or total protein unfolding, but rather the unfolding temperature of the area immediately surrounding the single Trp residue. The proteins used for these experiments were from the same samples that were used for the emission maxima scanning analyses. This ensured that the results seen or conclusions made, for these experiments, could be compared to the emission maxima data.

A sample series of temperature-dependent scans displays a single line for each temperature increment (2.5°C/scan) scanned from 305 nm to 400 nm. The temperature range scanned was from 10°C to 90°C (Figure 3.9). These data were then analyzed to determine the wavelength with the highest intensity (emission maximum). This wavelength was then graphed as a function of sample temperature (Figure 3.10).

The T_m given in this study is not a conventional T_m, as it is not referring to the unfolding of the entire protein, but rather the initial temperature at which the specific environment directly around a particular Trp residue begins to unfold. As with the emission maxima studies, this method is useful due to the natural fluorescent properties of the indole group contained in the Trp, which is directly influenced by its environment. First, the T_m of each IpaB only mutant will be compared to the T_m of the wildtype IpaB only Trp to determine difference in thermal stability of the regions containing a Trp. The wildtype 105W, without IpgC, has a T_m of 47°C (Table 3.4). When compared to the mutants without IpgC, only one (L133) has a lower T_m, indicating this region of the protein unfolds

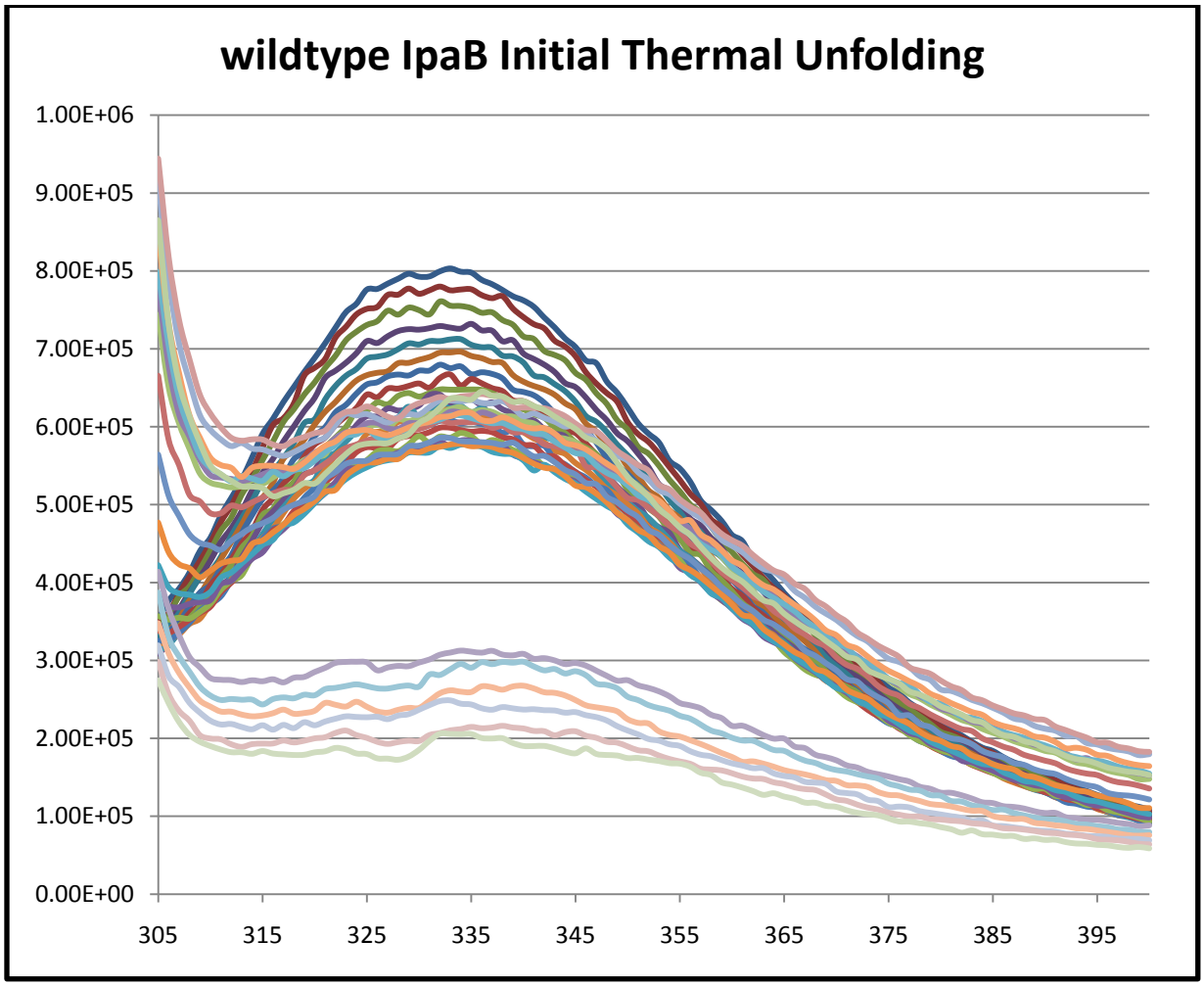

Figure 3.9 Initial Thermal Unfolding Graph of wildtype IpaB/IpgC Complex These data are analyzed as emission maximum versus temperature in Figure 3.10.

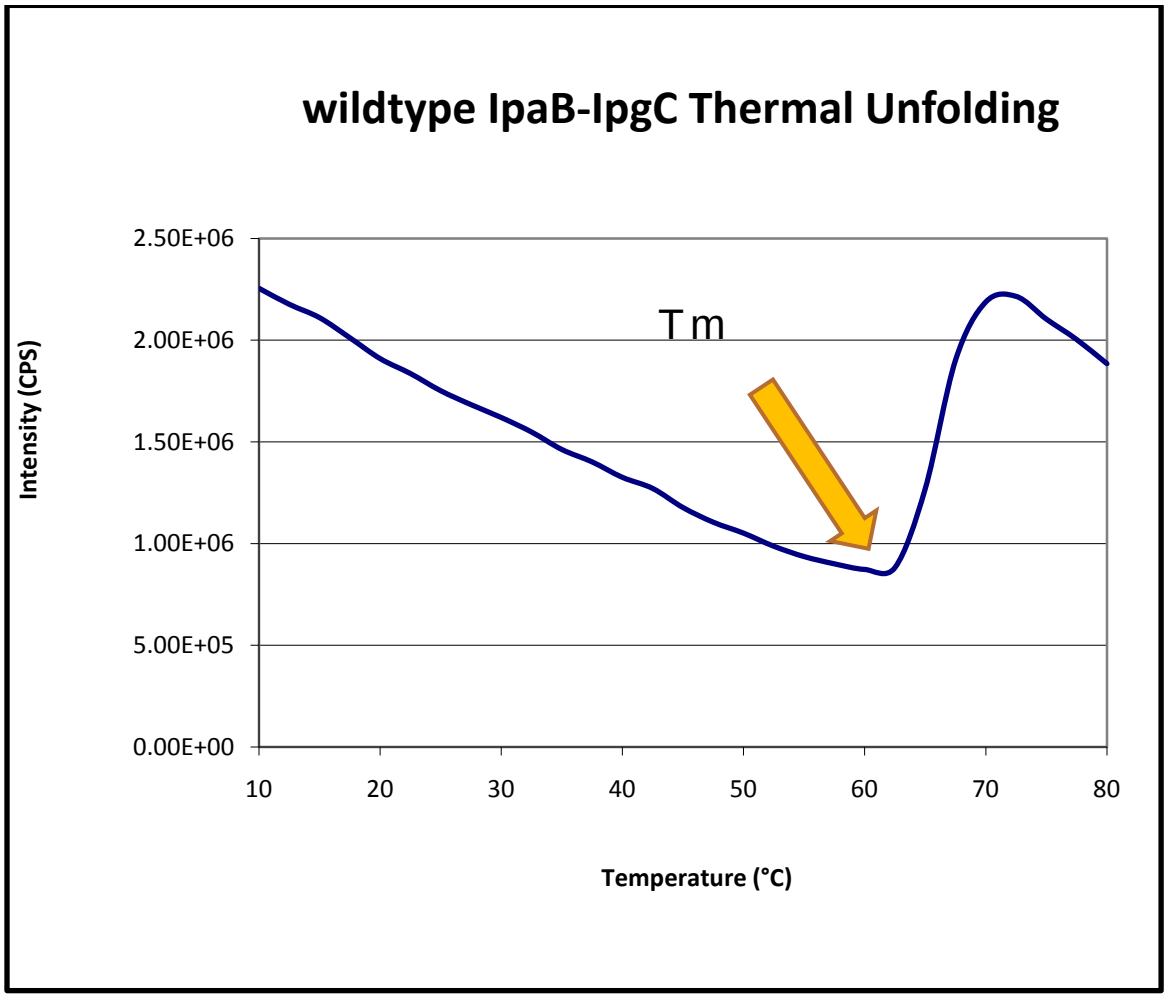

Figure 3.10 Thermal Unfolding Graph of wildtype IpaB/IpgC as a Function of Sample Temperature
The arrow shows the selected "transition" temperature which is considered the melting temperature or T_m of the area around a specific resiedue.

Trp Mutant	Melting Temp. (T_m), °C	ΔT_m[a], °C
IpaB/IpgC	61	
IpaB	47	-14
IpaB L79W/IpgC	68	
IpaB L79W	54	-14
IpaB F119W/IpgC	72.5	
IpaB F119W	55	-17.5
IpaB L133W/IpgC	66	
IpaB L133W	44	-22
IpaB D169W/IpgC	65	
IpaB D169W	52.5	-12.5
IpaB F275W/IpgC	55	
IpaB F275W	50	-5
IpaB Y293W/IpgC	52.5	
IpaB Y293W	52	-0.5
IpaB F382W/IpgC	70	
IpaB F382W	55	-15
IpaB F471W/IpgC	65	
IpaB F471W	55	-10
IpaB I553W/IpgC	54	
IpaB I553W	65	+9

Table 3.4 Thermal Unfolding of IpaB/IpgC Complex and IpaB Alone
T_m is not the melting point of the entire protein, but the point at which the environment around a specific Trp begins to unfold. [a]-Change in T_m of IpaB compared to IpaB/IpgC complex

before the region containing the native Trp. The other eight mutants all unfold at higher temperatures compared to the wildtype IpaB only, indicating that the area around these Trp residues unfolds later than the area around the native Trp.

Second the T_m of each mutant IpaB/IpgC complex will be compared to the T_m of the wildtype IpaB/IpgC complex to determine difference in the thermal stability of the regions that contain a Trp. The wildtype 105W IpaB/IpgC complex had a T_m of 61°C. When this result is compared to the IpaB/IpgC mutants, F275, Y293 and I553 display a lower T_m, indicating these three regions unfold before the region around the native Trp. The other six mutants displayed higher melting temperatures than the wildtype IpaB/IpgC complex, indicating that the regions containing those Trp residues unfold later than the region surrounding the native Trp.

Third, the T_m of the IpaB/IpgC complex will be compared to the T_m of IpaB only for each pair. The higher melting temperature of the wildtype IpaB/IpgC complex (61°C) compared to the T_m of the wildtype IpaB only (47°C) indicates that the region containing the native Trp in the IpaB/IpgC complex is more thermally stable when bound to IpgC than when not bound. Comparing the T_m of each mutant IpaB/IpgC complex to the T_m of its corresponding IpaB only mutants, eight had a higher T_m when bound to IpgC (Table 3.4). This indicates that the regions around these eight Trp residues are more stable and unfold at a higher temperature when IpaB is bound to IpgC. These data indicate that the overall effect of the binding of IpgC increases the thermal stability of IpaB.

One of the mutants, I553W, was the only sample in which the IpaB/IpgC complex was less thermally stable when compared to its corresponding IpaB only mutant. The I553W complex had an initial unfolding temperature of 54°C. I553W IpaB only had an initial unfolding temperature of 65°C, 11°C higher than its IpaB/IpgC complex. This Trp resides on the C-terminal coil or the second coil of the predicted dimeric coiled-coil. A possible reason for this decreased T_m is that the conformation imposed by the binding of IpgC on this region, which may be required for effective binding to IpgC, is less stable than the conformation when IpaB is ready to be secreted or interact with IpaC to form the translocon pore.

Three of the samples, wildtype IpaB, F471W and I553W, that displayed a significant temperature change when comparing the T_m of the IpaB/IpgC complex to IpaB alone, also displayed a significant shift in emission maximum when comparing their IpaB/IpgC complex to IpaB only. Wildtype IpaB is located in the predicted N-terminal helix-turn-helix; F471W is in the predicted transmembrane region nearest the C-terminus, while I553W is in the second coil of the dimeric coiled-coil. The large shifts seen at all three of these positions may indicate that the area around these three Trp residues might be heavily involved in the binding of IpgC, or may undergo a significant conformational change to facilitate the binding of IpgC. It is interesting to note that the two mutants with the largest change in initial unfolding temperature (T_m), F119W (-17.5°C) and L133W (-22°C), did not display a significant emission maximum shift, 2 nm blue shift and 1 nm red shift, respectively. These results suggest that these two regions are

stabilized by the binding of IpgC but they do not undergo a significant conformational change due to binding of IpgC.

Overall, the stability of the environments around the individual Trp residues is greater when IpaB is bound to its chaperone IpgC. These results were not entirely unexpected, since previous CD studies indicated that the IpaB/IpgC and the IpaC/IpgC complexes are more thermally stable compared to IpaB or IpaC alone (Birket *et al.*, 2007). However, CD spectroscopy measures global secondary structure while the fluorescence of a single Trp residue provides a snapshot of only a small microenvironment within the whole protein. In all samples but one, a significant T_m change was seen, which may indicate that all of these environments undergo a conformational change when bound to IpgC, increasing the amount of α-helices and β-sheets as shown by CD analysis, thereby increasing the thermal stability of the area around a single Trp and the protein as a whole (Birket *et al.*, 2007).

Förster Resonance Energy Transfer

Förster resonance energy transfer (FRET) is the nonradiative transfer of energy between a pair of fluorophores. After determining the amount of energy transferred from a donor to an acceptor it is possible to calculate the distance between the two fluorophores. When measuring the fluorescence of a single fluorophore, it is excited at a wavelength within its absorbance spectrum and it releases the absorbed energy as fluorescent light over a characteristic emission spectrum. If a second fluorophore is present whose absorbance overlaps the

emission spectrum of the first (donor) fluorophore, the excitation energy of the first can be passed to the second (acceptor) without the release of a photon. This is a distance-dependent phenomenon and FRET results in decreased (quenched) fluorescence of the donor probe.

To properly utilize FRET, it is important to determine the two fluorophores that will be used. The donor fluorophore emission spectrum must overlap with the excitation spectrum of the acceptor fluorophore (see Figure 3.11). The donor fluorophore can then be excited at a wavelength specific to it and not the acceptor fluorophore. In the absence of an acceptor probe, the donor will have a measurable amount of fluorescence. The fluorescence of the donor only sample is than compared to the fluorescence of the same donor in the presence of the acceptor (donor/acceptor sample). Decreased donor fluorescence intensity (quenching) will be seen as an increase in the donor/acceptor spectrum intensity, however, it is the donor quenching that is used to quantify FRET.

The donor probe in these experiments is the single Trp present in the wildtype or the mutant described above. To introduce an acceptor probe, the native single Cysteine (Cys) of IpaB at position 309 was labeled with a sufhydral reactive fluorophore. We chose to use 5-[2-[(2-Iodo-1-oxoethyl)amino] ethylamino]-1-naphthalenesulfonic acid (IAEDANS), to label Cys309. Cys309 is located at the end of the predicted first transmembrane helix. Because we know the positions of the newly introduced Trp residues we should be able to use FRET to determine a series of intramolecular distances to provide preliminary structural information of IpaB.

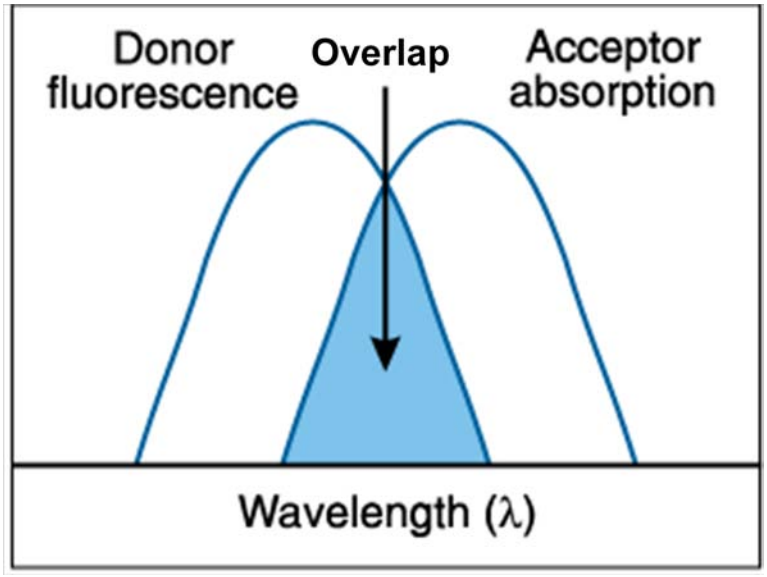

Figure 3.11 Principles of FRET
The donor emission fluorescence must overlap with the absorbance of the acceptor. This study used Trp as the donor and AEDANS as the acceptor.

Figure 3.12 displays the emission spectrum of wildtype IpaB consisting of the IpaB donor only sample (solid blue line) and the IpaB donor/acceptor (dashed red line) sample with the difference in FRET marked with an arrow. Results of all FRET spectra are shown in Table 3.5. To calculate the percent energy transferred between FRET pairs, the equation

$$(1-Fda/Fd) \text{ X } 100$$

was used, where Fd is the fluorescence emission maximum wavelength of the donor only sample and Fda is the fluorescence emission of the donor/acceptor sample at the same wavelength as the donor only sample. To calculate the distance between the two fluorophores, we used the equation

$$E=R_o^6/(R_o^6 + R^6)$$

where E equals the amount of energy transferred R_o is the theoretical distance that would give 50% FRET (R_o = 22Å for the Trp-AEDANS), and R equals the actual distance between the donor and acceptor in Å (Lakowicz, 2006). The distance measured was the distance from the Trp to the AEDANS molecule on Cys309, not directly to the Cys which introduces a modest amount of uncertainty to these distance calculations.

As can be seen in Table 3.5, all but one FRET pair had an amount of energy transfer between 50% and 90%. Only one sample had less than 50% energy transfer, IpaB F382W with 10.56%. F382W is located in the region predicted to lie on the inner face of the host cell membrane only 73 residues from Cys309. The data suggest this Trp at 382 is farther from the Cys309 than any of the other Trp residues. The other pairs are located closer together with

distances ranging from 15.44Å to 21.93Å. These data support the hypothesis that IpaB is a highly ordered molecule with a compact structure. We are still trying to convert these data into a topological map of IpaB.

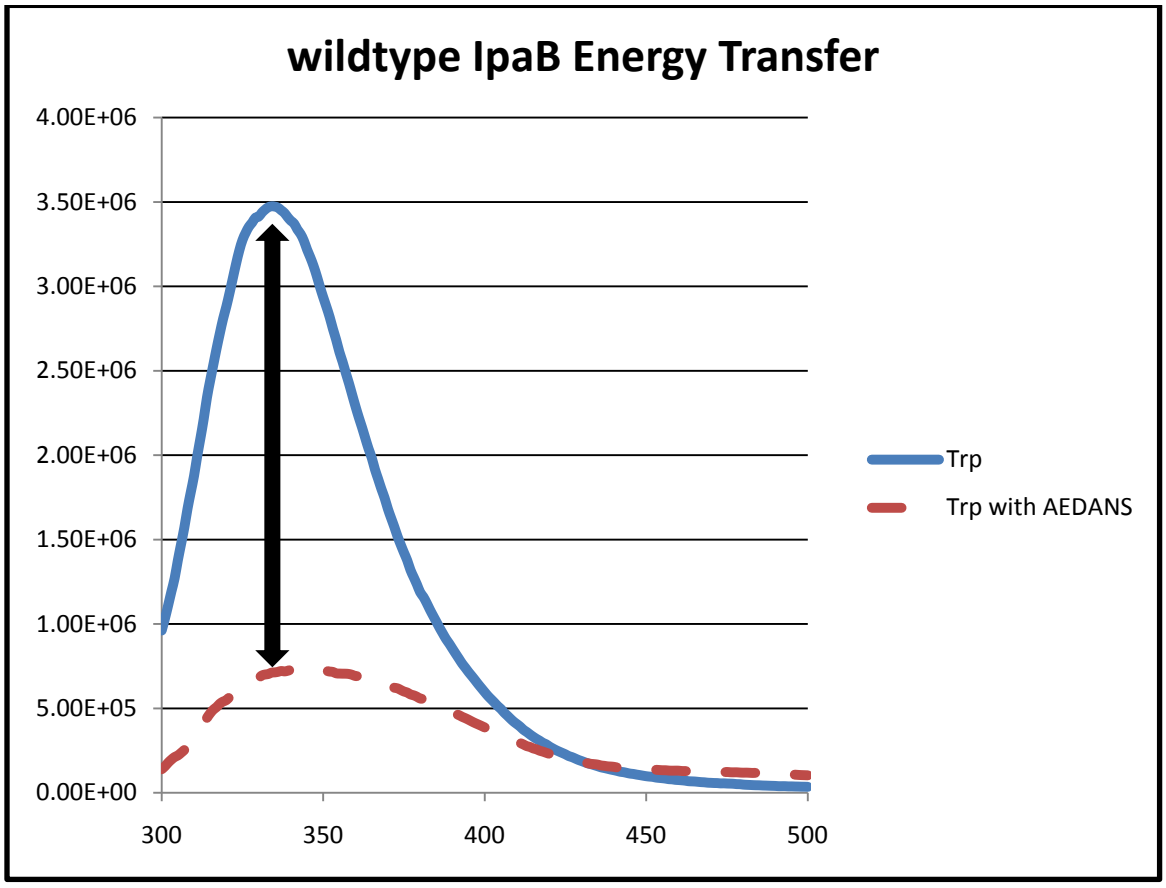

Figure 3.12 FRET Spectrum of wildtype IpaB
The emission spectrum of Trp is shown in the absence (solid blue line) and presence (dashed red line) of AEDANS acceptor. The black arrow shows the decrease in emission maximum for the IpaB donor/acceptor protein compared to the IpaB donor only protein.

Protein	Energy Transfer (%)	Calculated Distance (Å)
IpaB L79W	87.34	15.95
IpaB 105W	53.15	21.54
IpaB F119W	60.67	20.47
IpaB F133W	78.17	17.79
IpaB D169W	79.98	17.46
IpaB F275W	68.66	19.30
IpaB Y293W	89.32	15.44
IpaB F382W	10.56	31.41
IpaB F471W	89.18	15.48
IpaB I553W	50.49	21.93

Table 3.5 FRET of IpaB Trp Mutations
The percent energy transferred and calculated distance for each pair. The pairs consist of the Trp alone and the Trp plus the AEDANS labeled Cys309.

CHAPTER 4

DISCUSSION AND FUTURE PLANS

Shigella flexneri is the causative agent of shigellosis, a severe gastrointestinal disorder that is also called bacillary dysentery. It affects millions of people around the world every year. It is transmitted via the fecal-oral route and infects humans by invading the colonic epithelium. Once the bacterium has reached the colon, it takes advantage of microfold cells (M cells) that sample the environment of the colon to cross the epithelial layer (Owen, 1986). After entry, the bacterium is ingested by macrophages that are then induced to undergo apoptosis as *S. flexneri* secretes IpaB as an effector into their cytoplasm. *S. flexneri* is then released at the basal side of the epithelium, where it can then use its type III secretion system (TTSS) to induce ruffling of the host epithelial cells which leads to pathogen uptake by these cells. *Shigella* then escapes the resulting phagosome and grows in the host cell cytoplasm.

IpaB is secreted by the *Shigell*a TTSS to act as a structural protein, via interactions with IpaC, in the formation of a pore in the host cell membrane through which other late effectors can be directly injected into the host cell

cytoplasm to induce pathogen entry. Without IpaB, *S. flexneri* cannot escape the macrophage or form the pore to inject the effectors that induce cell ruffling in epithelial cells. Little research has been done that focuses on IpaB's structure. I hypothesize that IpaB is a highly structured and complex molecule, with and without its secretion chaperone IpgC, and that it is thermally more stable when bound to IpgC due to the stabilized conformation induced by its interaction with the IpgC chaperone. Tryptophan (Trp) scanning mutagenesis was used to better characterize the influence of IpgC on IpaB's structure. This hypothesis is supported by the data collected here and by FTIR and CD spectroscopy data that were performed elsewhere and generously made available for inclusion in this thesis. These data support the notion that IpaB has an intrinsic (intramolecular) dimeric coiled-coil and a significant α-helical structure.

This study focused on understanding the interactions of IpaB with its molecular chaperone, IpgC, and the structural effects imposed by the binding of IpgC by utilizing Trp scanning mutagenesis. Without its chaperone, IpaB could be lost or degraded prior to its secretion from *Shigella* as an effector or for formation of the translocon pore. This fluorescence study is possible because Trp has natural fluorescence properties that are greatly influenced by the immediate environment surrounding it. This approach allows monitoring of the microenvironments surrounding strategically-placed Trp residues within IpaB. By creating a library of single Trp containing point mutations we can study multiple regions throughout the length of the protein using the fluorescence properties of Trp. Initially, the wildtype IpaB and the twelve mutants were tested for invasion

and contact-hemolysis functions to determine if the mutations affected the function of the IpaB protein. The ΔW IpaB had the native Trp at residue 105 removed and replaced with phenylalanine (Phe). It showed no significant decrease in invasiveness or hemolysis suggesting that replacement of the original Trp does not affect the function of the protein. ΔW IpaB was not used for any fluorescence experiments since it lacks any Trp. The same functional assays were performed on all the single Trp mutants to determine the effect of the single Trp insertions on the function of the protein. Some displayed levels similar to the wildtype while several others displayed a decrease in virulence functions, which suggest that some of the residues replaced are needed for proper function of the protein. Overall these data suggest that the native Trp can be replaced and reintroduced in other locations without adversely affecting the IpaB's function. Insertions between residues 1 and 227 did not display a significant decrease in contact-mediated hemolysis while all the insertions past residue 227 displayed a significant decrease in hemolysis. This indicates that residues necessary for proper formation of the IpaB part of the translocon pore are located between 228 and 580. A similar result is seen for the invasion of cultured cells. These data may indicate that the portion of IpaB that is necessary for proper invasion is located in the transmembrane helices, the region that lies on the inner face of the host cell or the C-terminal coil of the dimeric coiled-coil. Three of the insertion mutants, F227W, I446W and F514W, were not found to express well. It was therefore decided that these three mutants would not be

used in subsequent experiments using purified IpaB. These three constructs will need to be remade in future studies.

To examine what is occurring at the protein level for these different IpaB mutants, the wildtype and single Trp mutant proteins were co-expressed with their IpgC chaperone in *E. coli* BL21 (DE3). They were then purified by Ni++ affinity chromatography using a His-tag located at the N-terminus of IpaB. IpaB was then separated from its chaperone IpgC using a mild detergent to study the effect of IpgC binding on IpaB's structure and functional properties. To determine areas that might be important for binding/interacting with IpgC the emission maximum of the various Trp residues in the IpaB/IpgC complex were compared to IpaB alone. Three comparisons were made, including a) comparing the emission maximum of the wildtype IpaB/IpgC complex to IpaB alone, b) the mutant IpaB/IpgC complex to the wildtype IpaB/IpgC complex, and c) comparing the IpaB only mutants to the IpaB only wildtype. In many cases, the Trp residues displayed a spectral shift to either the red or the blue during these comparisons. In some cases they displayed a significant spectral shift or a shift equal to or greater than 5 nm. Blue shifts in Trp residues indicate that the regions containing the Trp are becoming more hydrophobic (less polar) than the Trp to which it is being compared, possibly meaning the residues are more buried within the protein. Red spectral shifts indicate that the regions have become hydrophilic (more polar), possible meaning the residues are less buried or more exposed to the surrounding solvent. The reason for these shifts is likely due to either direct interaction with IpgC or these regions undergo a significant conformational

change induced by the binding of IpgC. We know IpgC is one third the size of IpaB. It is likely that IpgC induces IpaB to unfold or become less compact for proper binding, thus altering solvent exposure for some of the residues.

The emission maxima data also allow us to determine changes in the Trp-containing regions relative to the native Trp at residue 105. This includes whether these residues become more hydrophobic or hydrophilic (more or less polar) and whether they are more or less buried/exposed within the structure of IpaB. Relative to the native Trp105, we are able to say that residue L79 is more hydrophobic and more buried, F119 is very hydrophilic and more exposed, L133 is hydrophilic and more exposed, D169 is very hydrophilic and more exposed, F275 is more hydrophobic and less buried, Y293 is hydrophilic and more exposed, F382 is very hydrophobic and more buried, F471 is hydrophilic and more exposed, and I553 is hydrophobic and more buried with in the structure of IpaB. Most of the residues located near the transition between regions appear to be more exposed while the residues that lie in the interior of the predicted regions or the interior of the helices are more buried within the protein.

Fluorescence thermal unfolding analyses were used to monitor the stability of the various microenvironments containing the Trp residues and to demonstrate that most of the regions of IpaB are more thermally stable when bound to IpgC than when not bound to IpgC. The lone exception to this turned out to be I553W, whose lower T_m when bound to IpgC may be due to the conformation imposed on the region by IpgC binding (which may be necessary for proper binding to IpgC). It is possible that either a direct interaction of the Trp

or a nearby residue with IpgC causes the region to unfold earlier than when it is not bound to IpgC. There does not appear to be any correlation with the change in unfolding of a region and its environment with respect to hydrophobicity or hydrophilicity. Both types of environments display large and small thermal shifts in either direction. It does appear that the closer a residue is to a turn or a region joining two helices the larger the shift in thermal stability it displays. The reason for this is likely the same as with the emission maxima, that the region between the helices is less constrained and more likely to undergo a conformational change.

Förster resonance energy transfer studies allowed us to determine the amount of energy transferred between a specific Trp and the AEDANS, a probe linked to Cys309. This allowed us to calculate the distance between the donor and acceptor probes. Nine of the ten donor/acceptor pairs displayed 50% or more energy transfer indicating these Trp residues are 22Å or less away from Cys309. Only one residue appeared to lie further from Cys309 than 22Å. F382W appears to lie approximately 32Å away from Cys309, indicating that the region predicted to lie on the inner face of the host cell membrane protrudes from the protein unlike any of the other regions. This makes sense as this region is predicted to lie on the inner face of the host cell and it would thus need to protrude from the rest of the protein. Once a topological map of IpaB is developed using these data, we will be able to determine if IpaB does indeed fold similar to IpaD, another *S. flexneri* TTSS protein whose structure IpaB has been predicted to resemble.

Taken together, these data allow us to identify key regions/areas of IpaB induced in interactions with IpgC. They also lay the groundwork for determining the structure of IpaB. Key regions of IpaB may include the regions containing W105, F471 and I553, as each of these mutants displayed a significant spectral shift in emission maximum when the wildtype IpaB/IpgC complex was compared to the wildtype IpaB alone. This is expected as the three residues are predicted to be located in the loops or turns connecting the helices. Regions that connect helices tend to be more “floppy” or less constrained than the residues located within the helices. All three of these residues also displayed a significant shift in thermal stability in response to the binding or interaction with IpgC. It is interesting to note that two of the mutants that displayed a significant shift as a result of the binding of IpgC also had a complete loss of invasiveness and hemolysis indicating that the regions containing these insertions have undergone a change that disrupts the function of the protein. From the thermal unfolding analyses the regions containing F119, D169, Y293, and F382, are likely key regions as they undergo the largest shift in thermal stability indicating the binding of IpgC may have a greater effect on the conformation of these regions compared to the other regions of IpaB.

The hypothesis that IpaB is a highly structured and complex molecule that is more thermally stable when bound to its chaperone was supported by this work. Future plans would include further mutagenesis of the regions thought to be involved in IpgC binding to better characterize these interactions. The regions to be studied include the N-terminal helix-turn-helix between residues 1-78, the

N-terminal transmembrane helices between residues 170-227 and 228-274, the region predicted to lie on the inner face of the host cell membrane between residues 311-381, and the C-terminal coil between residues 554-580, because these regions appear to be the most affected by the binding of IpgC. This would increase our knowledge of the effects of IpgC binding on these areas. Cys mutants could be also made at the same locations as the Trp insertions, after removing and replacing the native Cys309, to allow complementery studies of IpaB by utilizing the same fluorescence experiments and measuring the distance between the Cys insertions and the wildtype Trp105 to further develop a model/topological map of IpaB.

REFERENCES

Alvarez-Martinez, C. E., and Christie, P. J., Biological Diversity of Prokaryotic Type IV Secretion Systems *Microbiol Mol Biol Rev* **73** (4), 775 (2009).

Alto, N.M., Shao, F., Lazar, C.S., Brost, R.L., Chua, G., Mattoo, S., McMahon, S.A., Ghosh, P., Hughes, T.R., Boone, C., and Dixon, J.E., Identification of a bacterial type III effector family with G protein mimicry functions *Cell* **124** (1),133 (2006).

Aubert, D. F., Flannagan, R. S., and Valvano, M. A., A novel sensor kinase-response regulator hybrid controls biolfilm formation and type VI secretion system activity in *Burkholderia cenocepacia Infect Immun* **76** (5), 1979 (2008).

Bahrani, F. K., Sansonetti, P. J., and Parsot, C., Secretion of Ipa proteins by *Shigella flexneri*: inducer molecules and kinetics of activation *Infect Immun* **65** (10), 4005 (1997).

Birket, S. E., Harrington, A. T., Espina, M., Smith, N. D., Terry, C. M., Darboe, N., Markham, A. P., Middaugh, C. R., Picking, W. L., Picking, W. D., Preparation and characterization of Translocator/Chaperone complexes and their component proteins from *Shigella flexneri Biochem* **46** (27), 8128 (2007).

Blocker, A., Gounon, P., Larquest, E., Niebuhr, K., Cabiaux, V., Parsot, C., and Sansonetti, P. J., The tripartite type III secretion of *Shigella flexneri* inserts IpaB and IpaC into host membranes *J Cell Biol* **147** (3), 683 (1999).

Blocker, A., Jouihri, N., Larquet, E., Gounon, P., Ebel, F., Parsot, C., Sansonetti, P., and Allaoui, A., Structure and composition of the *Shigella flexneri* "needle complex", a part of its type III secreton *Mol Microbiol* **39** (3), 652 (2001).

Buchrieser, C., Glaser, P., Rusniok, C., Nedjari, H., D'Hauteville, H., Kunst, F., Sansonetti, P., and Parsot, C., The virulence plasmid pWR100 and the repertoire of proteins secreted by the type III secretion apparatus of *Shigella flexneri Mol Microbiol* **38** (4), 760 (2000).

Cornelis, G. R., The type III secretion injectisome *Nat Rev Microbiol* **4** (11), 811 (2006).

Cornelis, G. R., and Van Gijsegem, F., Assembly and function of type III secretory systems *Annu Rev Microbiol* **54**, 735 (2000).

Davis, R., Marquat, M. E., Lucius, D., and Picking, W. D., Protein-protein interactions in the assembly of *Shigella flexneri* invasion plasmid antigens IpaB and IpaC into protein complexes *Biochem Biophys Acta* **1429** (1), 45 (1998).

DuPont, H. L., Levine, M. M., Hornick, R. B., and Formal, S. B., Inoculum size in shigellosis and implication for expected mode of transmission *J Infect Dis* **159** (6), 1126 (1989).

Epler, C. R., Dickenson, N. D., Olive, A. J., Picking, W. L., and Picking, W. D., Liposomes recruit IpaC to the *Shigella flexneri* type III secretion apparatus needle as a final step in secretion induction *Infect Immun* **77** (7), 2754 (2009).

Espina, M., Ausar, S.F., Middaugh, C.R., Baxter, M.A., Picking, W.D., Picking, W.L., Conformational stability and differential structural analysis of LcrV, PcrV, BipD, and SipD from type III secretion systems *Protein Sci* **16** (4), 704 (2007).

Espina, M., Olive, A. J., Kenjale, R., Moore, D. S., Ausar, S. F., Kaminski, R. W., Oaks, E. V., Middaugh, C. R., Picking, W. D., and Picking, W. L., IpaD localizes to the tip of the type III secretion system needle of *Shigella flexneri Infect Immun* **74** (8), 4391 (2006).

Flexner, S., On the etiology of tropical dysentery *Bull Johns Hopkings Hosp* **11**, 231 (1900).

Gerber, D. F., and Watkins, H. M., Growildtypeh of *shigellae* in monolayer tissue cultures *J Bacteriol* **82**, 815 (1961).

Guichon, A., Hersh, D., Smith, M.R., and Zychlinsky, A., Structure-function analysis of the *Shigella* virulence factor IpaB *J Bacteriol* **183** (4), 1269 (2001).

Handa, Y., Suzuki, M., Ohya, K., Iwai, H., Ishijima, N., Koleske, A. J., Fukui, Y., and Sasakawa, C., *Shigella* IpgB1 promotes bacterial entry through the ELMO-Dock180 machinery *Nat Cell Biol* **9** (1), 121 (2007).

Hale, T. L., Genetic basis of virulence in *Shigella* species *Microbiol Rev* **55**, 206 (1991).

Harper, J. R., and Silhavy, T. J., *Principles of Bacterial Pathogenesis*, edited by E. A. Groisman, 1st ed., Adademic Press, New York, NY, 2001.

Harrington, A., Darboe, N., Kenjale, R., Picking, W. L., Middaugh, C. R., Birket, S., and Picking, W. D., Characterication of the interaction of single tryptophan containing mutant of IpaC from Shigella flexneri with phospholipid membranes *Biochem* **45** (2), 626 (2006).

Hayward, R. D., Cain, R. J., McGhie, E. J., Phillips, N., Garner, M. J., and Koronakis, V., Cholesterol binding by the bacterial type III translocon is essential for virulence effector delivery into mammalian cells *Mol Microbiol* **56** (3), 590 (2005).

Hilbi, H., Modulation of phosphoinositide metabolism by pathogenic bacteria *Cell Microbiol* **8** (11), 1697 (2007).

Hilbi, H., Moss, J. E., Hersh, D., Chen, Y., Arondel, J., Banerjee, S., Flavell, R. A., Yuan, J., Sansonetti, P. J., and Zychlinsky, A., *Shigella*-induced apoptosis is dependent on caspase-1 which binds to IpaB *J Biol Chem* **273** (49), 32895 (1998).

Holland, I. B., Schmitt, L., and Young, J., Type 1 protein secretion in bacteria, the ABC-transporter dependent pathway (review) *Mol Membr Biol* **22** (1-2), 29 (2005).

Hueck, C. J., Type III protein secretion systems in bacterial pathogens of animals and plants *Microbiol Mol Biol Rev* **62** (2), 379 (1998).

Hume, P.J., McGhie, E.J., Hayward, R.D., and Koronakis, V., The purified *Shigella* IpaB and Salmonella SipB translocators share biochemical properties and membrane topology *Mol Microbiol* **49** (2), 425 (2003).

Islam, D., Bandholtz, L., Nilsson, J., Wigzell, H., Christensson, B., Agerberth, B., and Gudmundsson, G., Downregulation of bactericidal peptides in enteric infections: a novel immune escape mechanism with bacterial DNA as a potential regulator *Nat Med* **7** (2), 180 (2001).

Islam, D., Veress, B., Bardhan, P.K., Lindberg, A. A., and Christensson, B., In situ characterization of inflammatory responses in the rectal mucosae of patients with shigellosis *Infect Immun* **65** (2), 739 (1997).

Jacob-Dubuisson, F., Fernandez, R., and Coutte, L., Protein secretion through autotransporter and two-partner pathways *Biochim Biophys Acta* **1694** (1-3), 235 (2004).

Klauser, T., Krämer, J., Otzelberger, K., Pohlner, J., and Meyer, T. F,. Characterization of the *Neisseria* Iga beta-core. The essential unit for outer membrane targeting and extracellular protein secretion *J Mol Biol* **234** (3), 579 (1993).

Krieg, N. R., and Holt, J. G., Family I. Enterobacteriaceae. *Bergey's manual of systematic bacteriology* **1**, 408 (1984).

Kruse, W., Ueberdie Ruhr als Volkskrankheit und ihrer erreger. *Dtsch. Med Wocherschr* **26**, 637 (1900).

Kueltzo, L. A., Osiecki, J., Barker, J, Picking, W. L., Ersoy, B., Picking, W. D., and Middaugh, C. R., Structure-function analysis of invasion plasmid antigen C (IpaC) form *Shigella Flexneri J Biol Chem* **278** (5), 2792 (2003).

Labrec, E.H., Schneider, H., Magnani, T.J., and Formal, S.B., Epithelial Cell Penetration as an Essential Step in the Pathogenesis of Bacillary Dysentery *J Bacteriol* **88** (5), 1503 (1964).

Lakowicz, J. R., *Principles of Fluorescence Spectroscopy,* 3rd ed., Springer, New York, NY, 2006.

Lunelli, M., Lokareddy, R. K., Zychlinsky, A., and Kolbe, M., IpaB/IpgC interaction defines binding motif for type III secretion translocator *Proceed Nat Acdmy Sci* **106** (24), 9661 (2009).

Mavris, M., Page, A.L., Tournebize, R., Demers, B., Sansonetti, P., and Parsot, C., Regulation of transcription by the activity of the *Shigella flexneri* type III secretion apparatus *Mol Microbiol* **43** (6). 1543 (2002).

Maurelli, A. T., Baudry, B., d'Hauteville, H., Hale, T. L., and Sansonetti, P. J., Cloning of plasmid DNA sequences involved in invasion of HeLa cells by *Shigella flexneri Infect Immun* **49** (1), 164 (1985).

Menard, R., Sansonetti, P. J., and Parsot, C., Nonpolar mutagenesis of the ipa genes defines IpaB, IpaC, and IpaD as effectores of *Shigella flexneri* entry into epithelial cells *J Bacteriol* **175** (18), 5899 (1993).

Menard, R., Sansonetti, P., and Parsot, C., The secretion of the *Shigella flexneri* Ipa invasions is activated by epithelial cells and controlled by IpaB and IpaD *Embo J* **13** (22), 5293 (1994).

Menard, R., Sansonetti, P., Parsot, C., and Vasselon, T., Extracellular association and cytoplasmic partitioning of the IpaB and IpaC invasions of *S. flexneri Cell* **79** (3), 515 (1994).

Mounier, J., Vasselon, T., Hellio, R., Lesourd, M., and Sansonetti, P. J., *Shigella flexneri* enters human colonic Caco-2 epithelial cells through the basolateral pole *Infect Immun* **60** (1), 237 (1992).

Niebuhr, K. Giuriato, S., Pedron, R., Philpott, D. J., Gaits, F., Sable, J., Sheetz, M. P., Parsot, C., Sansonetti, P. J., and Payrastre, B., Conversion of PtdIns(4,5)P(2) into PtdIns(5)P by the *S. flexneri* effector ipgD reorganizes host cell morphology *Embo J* **21** (19), 5069 (2002).

Niyogi, S. K., Shigellosis *J Microbiol* **43** (2), 133 (2005).

O'Brien, A. D., LaVeck, G. D., Griffin, D. E., and Thompson, M. R., Characterization of *Shigella dysenteriae* 1 (Shiga) toxin purified by anti-Shiga toxin affinity chromatography *Infect Immun* **30** (1), 170 (1980).

Olive, A. J., Kenjale, R., Espina, M., Moore, D. S., Picking, W. L., and Picking W. D., Bile salts stimulate recruitment of IpaB to the *Shigella* flexneri surface, where it colocalizes with IpaD at the tip of the type III secretion needle *Infect Immun* **75** (5), 2626 (2007).

Owen, R. L., Pierce, N. F., Apple, R. T., and Cray, W. C. Jr., M cell transport of *Vibrio cholerae* from the intestinal lumen into Peyer's patches: a mechanism for antigen sampling and for microbial transepithelial migration *J Infect Dis* **153** (6), 1108 (1986).

Paetzold, S., Lourido, S., Raupach, B., and Zychlinsky, A., *Shigella flexneri* phagosomal escape is independent of invasion *Infect Immun* **75** (10), 4826 (2007).

Page, A. L., Ohayon, H., Sansonetti, P. J., and Parsot, C., The secreted IpaB and IpaC invasions and their cytoplasmic chaperone IpgC are required for intercellular dissemination of *Shigella flexneri Cell Microbiol* **1** (2), 183 (1999).

Page, A. L., Fromont-Racine, M., Sansonetti, P., Legrain, P., and Parsot, C., Characterization of the interaction partners of secreted proteins and chaperones of *Shigella flexneri Mol Microbiol* **42** (4), 1133 (2001).

Parsot, C., Menard, R., Gounon, P., and Sansonetti, P. J., Enhanced secretion through the *Shigella flexneri* Mxi-Spa translocon leads to assemble of extracellular proteins into macromolecular structures *Mol Microbiol* **16** (2), 291 (1995).

Parsot, C., Hamiaux, C., and Page, A.L., The various and varying roles of specific chaperones in type III secretion systems *Curr Opin Microbiol* **6** (1), 7 (2003).

Parsot, C., Ageron, E., Penno, C., Mavris, M., Jamoussi, K., d'Hauteville, H., Sansonetti, P., and Demers, B., A secreted anti-activator, OspD1, and its chaperone, Spa15, are involved in the control of transcription by the type III secretion apparatus activity in *Shigella flexneri Mol Microbiol* **56** (6),1627 (2005).

Phalipon, A., and Sansonetti, P. J., *Shigella's* ways of manipulating the host intestinal innate and adaptive immune system: a tool box for survival? *Immuno Cell Biol* **85** (2), 119 (2007).

Phalipon, A., Mulard, L. A., and Sansonetti, P. J., Vaccination against shigellosis: is it the path that is difficult or is it the difficult that is the path? *Microbes Infect* **10** (9), 1057 (2008).

Picking, W.L., Mertz, J.A., Marquart, M.E., Picking, W.D., Cloning, expression, and affinity purification of recombinant Shigella flexneri invasion plasmid antigens IpaB and IpaC *Protein Expr Purif* **8** (4), 401 (1996).

Picking, W.L., Coye, L., Osiecki, J.C., Barnoski Serfis, A., Schaper, E., and Picking, W.D., Identification of functional regions within invasion plasmid antigen C (IpaC) of *Shigella flexneri Mol Microbiol* **39** (1), 100 (2001).

Picking, W. L., Nishioka, H., Hearn, P. D., Baxter, M. A., Harrington, A. T., Blocker, A., and Picking, W. D., IpaD of *Shigella flexneri* is independently required for regulation of Ipa protein secretion and efficient insertion of IpaB and IpaC into host membranes *Infect Immun* **73** (3), 1432 (2005).

Pilonieta, M.C., and Munson, G.P., The chaperone IpgC copurifies with the virulence regulator MxiE *J Bacteriol* **190** (6), 2249 (2008).

Purdy, G. E., Fisher, C. R., Payne, S. M., IcsA surface presentation in *Shigella flexneri* requires the periplasmic chaperones DegP, Skp, and SurA *J Bacteriol* **189** (15), 5566 (2007).

Pukatzki, S., Ma, A. T., Sturtevant, D., Krastins, B., Sarracino, D., Nelson, W. C., Heidelberg, J. F., and Mekalanos, J. J., Identification of a conserved bacterial protein secretion system in *Vibrio cholerae* using the *Dictyostelium* host model system *Proc Natl Acad Sci* **103** (5), 1528 (2006).

Russel, M., Macromolecular assembly and secretion across the bacterial cell envelope: Type II protein secretion systems *J Mol Biol* **279**, 485 (1998).

Sams, C. F., Friedman, E. B., Burgum, A. A., Yang, D. S., and Matthews, K. S., Spectral Studies of Lactose Repressor Protein Modified with Nitrophenol Reporter Groups *Journ Biological Chem* **252** (10), 3153 (1977).

Sansonetti, P. J., Arondel, J., Cantey, R., Prevost, M. C., and Huerre, M., Infection of rabbit Peyer's patches by *Shigella flexneri*: effect of adhesive or invasive bacterial phenotypes on follicle-associated epithelium *Infect Immun* **64** (7), 2752 (1996).

Sansonetti, P. J., d'Hauteville, H., Formal, S. B., and Toucas, M., Plasmid-mediated invasiveness of "*Shigella*-like" *Escherichia coli Ann Microbiol (Paris)* **133** (3), 351 (1982).

Sansonetti, P. J., Kopecko, D. J., and Formal, S. B., *Shigella sonnei* plasmids: evidence that a large plasmid is necessary for virulence *Infect Immun* **34** (1), 75 (1981).

Sansonetti, P. J. Kopecko, D. J., and Formal, S. B., Involvement of a plasmid in the invasive ability of *Shigella flexneri Infect Immun* **35** (3), 852 (1982).

Sansonetti, P. J., Phalipon, A., Arondel, J., Thrumalai, K., Banerjee, S., Akirn, S., Takeda, K., and Zychlinsky, A., Caspase-1 activation of IL-1 beta and IL-18 are essential for *Shigella flexneri*-induced inflammation *Immunity* **12** (5), 581 (2000).

Sansonetti, P.J., Ryter, A., Clerc, P., Maurelli, A.T., and Mounier, J., Multiplication of *Shigella flexneri* within HeLa cells: lysis of the phagocytic vacuole and plasmid-mediated contact hemolysis *Infect Immun* **51** (2), 461 (1986).

Schroeder, G. N. and Hilbil, H., Molecular pathogenesis of *Shigella* spp.: controlling host cell signaling, invasion, and death by type III secretion *Clin Microbiol Rev* **21** (1), 134 (2008).

Sereńy, B., Experimental keratoconjunctivitis Shigellosa *Acta Microbiol Acad Sci Hung* **4** (4), 367 (1957).

Shiga, K., Sekiri byogen kenkyu hokoku dia-ichi (first report on etiologic research of dysentery) *Saikingaku Zasshi* **25** (1), 790 (1897).

Shiga, K., Observation on the epidemiology of dysentery in Japan *Philippine J of Sci* **1**, 485 (1906).

Stensrud, K.F., Adam, P.R., La Mar, C.D., Olive, A.J., Lushington, G.H., Sudharsan, R., Shelton, N.L., Givens, R.S., Picking, W.L., and Picking, W.D., Deoxycholate interacts with IpaD of Shigella flexneri in inducing the recruitment of IpaB to the type III secretion apparatus needle tip *J Biol Chem* **283** (27),18646 (2008).

Sur, D., Ramamurthy, T., Deen, J., and Bhattacharya, S. K., Shigellosis: challenges & management issues *Indian J Med Res* **120**, 454 (2004).

Takeuchi, A., Electron microscope studies of experimental *Salmonella* infection. I. Penetration into the intestinal epithelium by *Salmonella typhimurium Am J Pathol* **50** (1), 109 (1967).

Terry, C. M., Picking, W. L., Birket, S. E., Flentie, K., Hoffman, B. M., Barker, J. R., and Picking, W.D. The C-terminus of IpaC is required for effector activities related to *Shigella* invasion of host cells *Microb Pathog* **45** (4), 282 (2008).

Tran Van Nhieu, G., Caron, E., Hall, A., and Sansonetti, P. J., IpaC induces actin polymerization and filopodia formation during *Shigella* entry into epithelial cells *Embo J* **18** (12), 3249 (1999).

van der Goot, F.G., Tran van Nhieu, G., Allaoui, A., Sansonetti, P., and Lafont, F., Rafts can trigger contact-mediated secretion of bacterial effectors via a lipid-based mechanism *J Biol Chem* **279** (46), 47792 (2004).

Watanabe, H., Arakawa, E., Ito, K., Kato, J., and Nakamura, A., Genetic analysis of an invasion region by use of a Tn3-lac transposon and identification of a second positive regulator gene, invE, for cell invasion of *Shigella sonnei*: significant homology of invE with ParB of plasmid P1 J Bacteriol 172 (2), 619 (1990).

Wassef, J. S., Keren, D. F., and Mailloux, J. L., Role of M cells in initial antigen uptake and in ulcer formation in the rabbit intestinal loop model of shigellosis *Infect Immun* **57** (3), 858 (1989).

Watarai, M., Tobe, T., Yoshikawa, M., and Sasakawa, C., Contact of *Shigella* with host cells triggers release of Ipa invasions and is an essential function of invasiveness *Embo J* **14** (11), 2461 (1995).

Watkins, H. M., Some attributes of virulence in *Shigella Ann N Y Acad Sci.* **88**, 1167 (1960).

Winans, S. C., Burns, D. L., and Christie, P. J., Adaptation of a conjugal transfer system for the export of pathogenic molecules *Trends Microbiol* **4**, 64 (1996).

Yoshida, S., Handa, Y., Suzuki, T., Ogawa, M., Suzuki, M., Tamai, A., Abe, A., Katayama, E., and Sasakawa, C., Microtubule-severing activity of *Shigella* is pivotal for intercellular spreading *Science* **314** (5801), 985 (2006).

Yoshikawa, M., Saskawa, C., Makino, S., Okada, N., Lett, M. C., Sakai, T., Yamada, M., Komatsu, K., Kamata, K., Kurata, T., and *et al.*, Molecular genetic approaches to the pathogenesis of bacillary dysentery *Microbiol Sci* **5** (11), 333 (1988).

Zheng, J., and Leung, K. Y., Dissection of a type VI secretion system in *Edwardsiella tarda Mol Microbiol* **66** (5), 1192 (2007).

Zychlinsky, A., Kenny, B., Menard, R., Prevost, M. C., Hooand, I. B., and Sansonetti, P. J., IpaB mediates macrophage apoptosis induced by *Shigella flexneri Mol Micrbiol* **11** (4), 619 (1994).

VITA

Christopher Michael Sheehan

Candidate for the Degree of

Master of Science

Thesis: SECONDARY STRUCTURAL ANALYSIS OF *SHIGELLA FLEXNERIA* INVASION PLASMID ANTIGEN B (IPAB)

Major Field: Microbiology

Biographical:

Personal Data:

Christopher Michael Sheehan
620 S. Broad
Guthrie, OK 73044

Education:

Completed the requirements for the Master of Science in Microbiology at Oklahoma State University, Stillwater, Oklahoma in May, 2010.

Completed the requirements for the Bachelor of Science in Microbiology at Oklahoma State University, Stillwater, OK in May 2007.

Experience:

Working with Dr. Wendy Picking on the secondary structure analysis of IpaB of *Shigella flexneri* since June of 2009.

Working with Dr. Anand Sukhan on the molecular and genetic analysis of the mechanisms of type III secretion in the bacterial pathogens *Pseudomonas aeurginosa* and *Escherichia coli* from August 2006 to May 2006.

Professional Memberships:

America Society for Microbiology

Name: Christopher Michael Sheehan Date of Degree: May, 2010

Institution: Oklahoma State University Location: Stillwater, Oklahoma

Title of Study: SECONDARY STRUCTURAL ANALYSIS OF *SHIGELLA FLEXNERIA* INVASION PLASMID ANTIGEN B (IPAB)

Pages in Study: 112 Candidate for the Degree of Master of Science

Major Field: Microbiology

Scope and Method of Study:
This study focuses on the secondary structure of invasion plasmid antigen B (IpaB) of *Shigella flexneri* and the effects on it by the binding of invasion plasmid gene C (IpgC) along with sites of interaction with IpgC. IpgC is the molecular chaperone of IpaB that is responsible for keeping IpaB from associating with invasion plasmid antigen C (IpaC) or degrading before it is secreted. A library of single tryptophan containing mutants was created by replacing the native tryptophan (Trp) at position 105 with phenylalanine (Phe) and using this as a template to make twelve mutants by inserting Trp at places throughout the length of the protein. Fluorescence spectroscopy utilizing the naturally fluorescent properties of Trp was used to determine areas of interaction with IpgC and the effects of IpgC's binding on IpaB's secondary structure and topology.

Findings and Conclusions:
Invasion and hemolysis assays showed that the native Trp at residue 105 could be replaced with Phe and used as a template to make single insertion mutants. The same assays showed that several of the mutants had no effect on the protein's function while some of the mutants showed no invasiveness or hemolysis but no significant structural changes. Three mutants were determined to be problematic and their use was discontinued. The emission maximum scans showed that many of the mutants were not affected by the binding of IpgC. Two mutants plus the wildtype IpaB displayed significant spectral shifts to the red, indicating that the environment around that Trp became more polar (more hydrophilic) when not bound to IpgC. The thermal unfolding analysis showed that IpaB was more stable when in complex with IpgC than when alone except in one case (for the mutant I553W). The Förster resonance energy transfer (FRET) studies provided information to determine the tertiary structure features of IpaB. These data support the hypothesis that IpaB is a highly structured and complex molecule that is more thermally stable when bound to its chaperone IpgC.

ADVISER'S APPROVAL: Dr. Wendy Picking